melanoma cells into the opposite flank. Tumor volumes were calculated at day 14 after the second transplantation of B16 melanoma cells.

2.4.2. Protocol Number 2: Effect of Treatment Frequency with NPrCAP/M on Re-Challenge Tumor Growth. Mice were randomly divided into six treatment groups. They were exposed to AMF once on day 6 (Group I), twice (on days 6 and 8) (Group II), twice (on days 6 and 10) (Group III), three times (on days 6, 8, and 10) (Group IV), three times (on days 6, 7, and 8) (Group V), and five times (on days 6 through 10) (Group VI).

2.4.3. Protocol Number 3: Effect of Temperature and Treatment Frequency of NPrCAP/M with AMF on Re-Challenge Tumor Growth. Mice were divided into six groups. Mice of Groups I and II were exposed to the AMF to maintain the surface temperature at 41°C once a day for two days (days 6 and 10) and for three days (days 6, 8, and 10), respectively. Using the same day schedule mice of Groups III and IV were exposed to the AMF at 43°C and mice of Groups V and VI at 46°C.

2.4.4. Protocol Number 4: Effect of Temperature and Treatment Duration on Re-Challenge Tumor Growth. Mice were divided into four groups. Temperatures at the surface of the tumors in Groups I and II were maintained at 43°C and 46°C, respectively, during AMF exposure for 15 minutes. The surface temperatures in Groups III and IV were maintained at 43°C and 46°C, respectively, during therapy for 30 minutes.

2.5. ELISA for Heat Shock Protein 70 (HSP70) Expression in a Tumor. After thermotherapy, the amount of HSP70 in the primary tumor was measured using an HSP70 EIA Kit (Stress Gen Biotechnologies, British Columbia, Canada) according to the manufacturer's instructions. The total protein content of the tumor homogenates was determined using the BCA Protein Assay Kit (Pierce Biothechnology, Inc., USA). The control group was composed of mice without NPrCAP/M administration or AMF exposure. Group I received *s.c.* administration of NPrCAP/M directly at the tumor site once a day without AMF exposure. Mice of Groups II and III received thermotherapy at 41°C for 15 minutes and 30 minutes, Groups IV and V at 43°C for 15 minutes and 30 minutes, and Groups VI and VII at 46°C for 15 minutes and 30 minutes, respectively. Then, 24 hours later, all tumors were removed, and their lysates were processed for the HSP70 assay. In separate groups, tumors were excised at 24, 48, and 72 hours after the 43°C thermotherapy for 30 minutes, and amounts of HSP70 were measured.

2.6. Histological and Immunohistochemical Study. After thermotherapy in the primarily transplanted melanoma at 43°C for 30 minutes once a day for three days (Figure 4(a), Group IV), melanomas in re-challenge mice were excised on the 18th day after second transplantation of B16F1 cells. Paraffin-embedded sections were prepared and processed for HE staining. The frozen tumor tissues were stained with antimouse CD4 (Santa Cruz Biotechnology Inc., CA, USA) or CD8 (Chemicon International Inc., CA, USA).

2.7. Statistical Analysis. Data were analyzed by one- or two-way analysis of variance (ANOVA), and then differences in experimental results for tumor growth and expression of HSP were assessed by Sheffe's test to compare all the experimental groups, or by Dunnett's test, which compared the experimental versus the control groups. Differences in survival rates were analyzed by the Kaplan-Meier method and log-rank test with Bonferroni correction for multiple comparisons. The level of significance was $P < .05$ (two-tailed). All statistical analyses were performed using Stat View J-5.0 (SAS Institute Inc. Cary, NC).

3. Results and Discussion

In the search for successful cancer treatment it is self-evident that the exploitation of a specific biological property is one of the best approaches for developing the targeted therapy [27, 28]. We have previously shown that the melanogenesis substrate, NPrCAP, is a good candidate for developing melanoma chemotherapy because melanogenesis is uniquely expressed in melanocytic cells and is inherently cytotoxic from the action of tyrosinase on tyrosine with formation of highly reactive free radicals [1, 4]. Nanoparticles may also provide a good platform to coadminister anticancer therapeutics directed at different targets. Specifically hyperthermia with the use of magnetite nanoparticles has been shown to possess great potential to develop thermo-immunotherapy [23, 29]. In this study the conjugate of NPrCAP and magnetite nanoparticles, NPrCAP/M was synthesized with the hope of developing a chemotherapeutic as well as a thermo-immunotherapeutic effect. We employed two cell lines of B16 melanoma, that is, B16F1 and B16F10, and B16OVA cells and compared the thermo-therapeutic protocols in detail by evaluating the growth of the re-challenge melanoma as well as the duration and rates of survival of melanoma-bearing mice.

3.1. Immediate and Steady Generation of Heat by Intratumor Administration of NPrCAP/M with AMF Exposure on B16 Melanoma Nodules. In the previous intratumor MCL hyperthermia for B16 melanoma the skin surface temperature above the subcutaneous tumor rose to 43 or 46°C [29]. To obtain a rapid and steady temperature increase at the core and the surface of the B16 melanoma, NPrCAP/M was injected into the center of the tumor nodules, and internal and surface tumor temperatures were measured during AMF exposure. Both temperatures increased within one minute to the target of 41°C, 43°C, or 46°C (Figures 1(a), 1(b), and 1(c)), indicating that NPrCAP/M injection followed by AMF exposure could immediately and steadily heat the subcutaneously transplanted melanoma nodules. The temperature at the tumor center was approximately 2°C higher than that at the tumor surface.

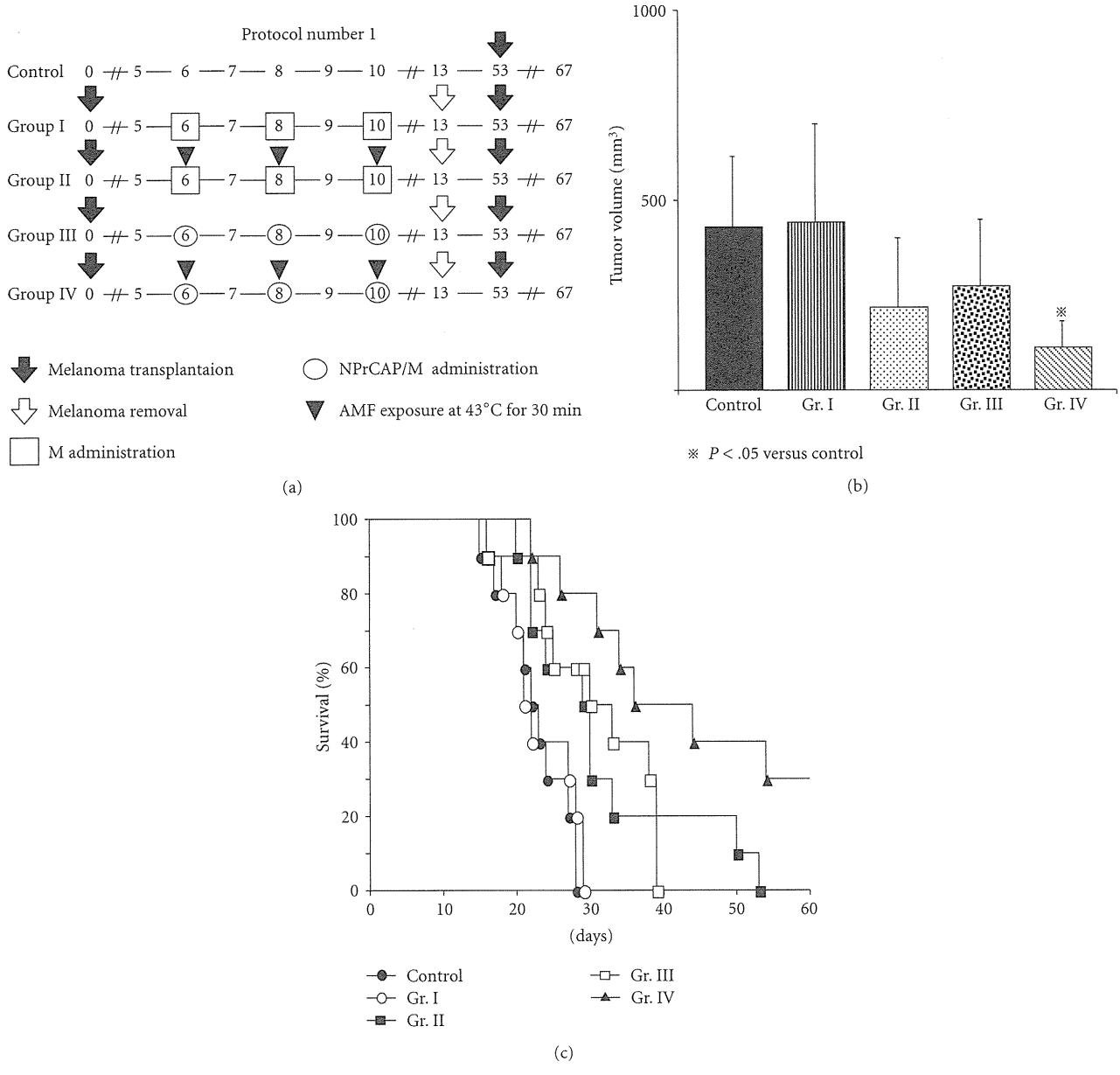

FIGURE 3: Time schedules and results for tumor volumes, survival periods, and rates of mice treated by the Protocol number 1. (a) Protocols of Groups I, II, III, and IV. (b) Tumor volumes of re-challenge B16F1 melanoma on day 14. All data are presented as mean ± standard deviation. Tumor volumes of Group IV were significantly reduced compared with those of the control group (P = .0295) or Group I (P = .0215). There were no significant interactions between drugs and AMF (P = .5568). (c) Kaplan-Meier survival curve over a period of 60 days after tumor re-challenge in Protocol number 1.

3.2. Effective and Equal Inhibition of B16 Melanoma Growth at the Site of Primary Transplantation by Intratumor Administration of NPrCAP/M with and without Heat. We first evaluated the chemotherapeutic effect of NPrCAP/M with or without heat. NPrCAP/M without heat inhibited the growth of primary transplants to the same degree as did NPrCAP/M with heat, indicating that NPrCAP/M alone has a chemotherapeutic effect. The critical temperature for thermotherapy was documented to be 43°C for various cell lines [7, 8]. Using two melanoma cell lines, B16F1, and B16F10 and B16OVA, we examined melanoma growth inhibition by intra-tumor administration of NPrCAP/M into primary tumors on days 6, 8, and 10 after transplantation with exposure to AMF at 43°C for 30 minutes (Figures 2(a) and 2(c)) under the experimental conditions of Protocol number 1 (Figure 3(a)). Both NPrCAP/M with and without AMF exposure resulted in a significant and equal reduction of melanoma tumor volume in both B16F1 and F10 cells

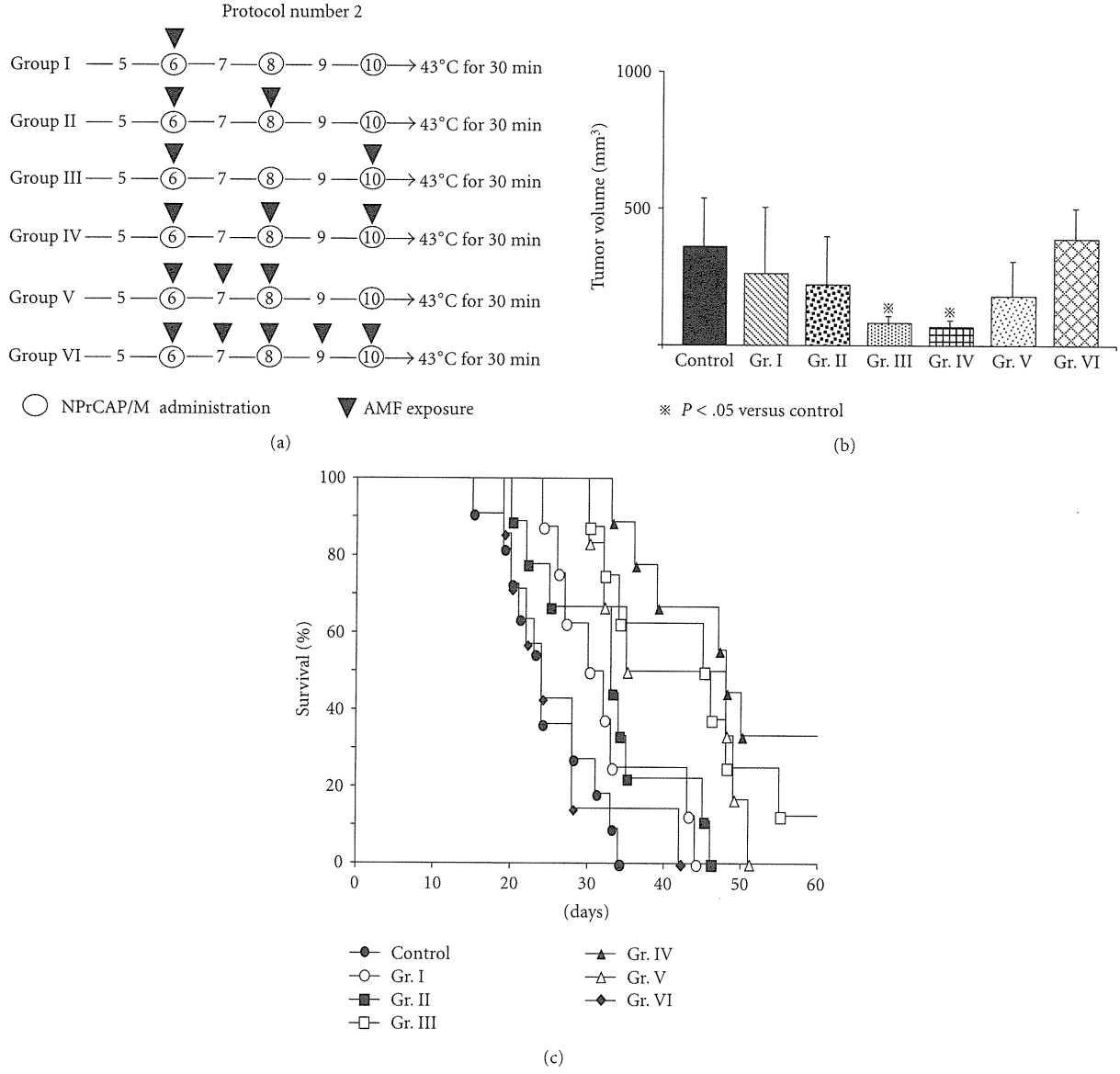

FIGURE 4: Time schedule and results for tumor volumes, survival periods, and rates of mice treated by Protocol number 2. (a) Protocols of Groups I, II, III, IV, V, and VI. (b) Tumor volumes on day 14 after re-challenge with B16F1 melanoma. All data are presented as mean ± standard deviation. Tumor volumes of Groups III and IV were found to be significantly reduced compared with those of the control group ($P = .0411$ and .0195, resp.) and Group VI ($P = .0444$ and .0237, resp.) by the Scheffé test. (c) Kaplan-Meier survival curves over a period of 60 days after re-challenge with B16F1. The survival rate of Group III was significantly prolonged compared with those of the control group ($P = .0006$) and Group VI ($P = .0013$). The survival rate of Group IV was significantly prolonged compared with that of the control group ($P < .0001$), Group I ($P = .0014$), Group II ($P = .0014$), and Group VI ($P = .0013$). One of the eight mice in Group III and three of the nine mice in Group IV were protected against re-challenge with B16F1 melanoma cells.

at the site of primary transplantation ($P < .01$ by two-way repeated measure ANOVA, Figures 2(a) and 2(c)) compared to tumor volume of naive control mice. B16 OVA cells also gave the same experimental results (data not shown). Control studies comparing magnetite alone and magnetite plus NPrCAP (NPrCAP/M) without AMF exposure showed that magnetite alone does not have any melanoma growth inhibiting effect whereas NPrCAP/M without AMF significantly inhibited melanoma-growth ($P < .01$ by two-way repeated measure ANOVA, Figure 2(b)). Since we obtained basically same growth inhibition results for both the primary and secondary transplants from the

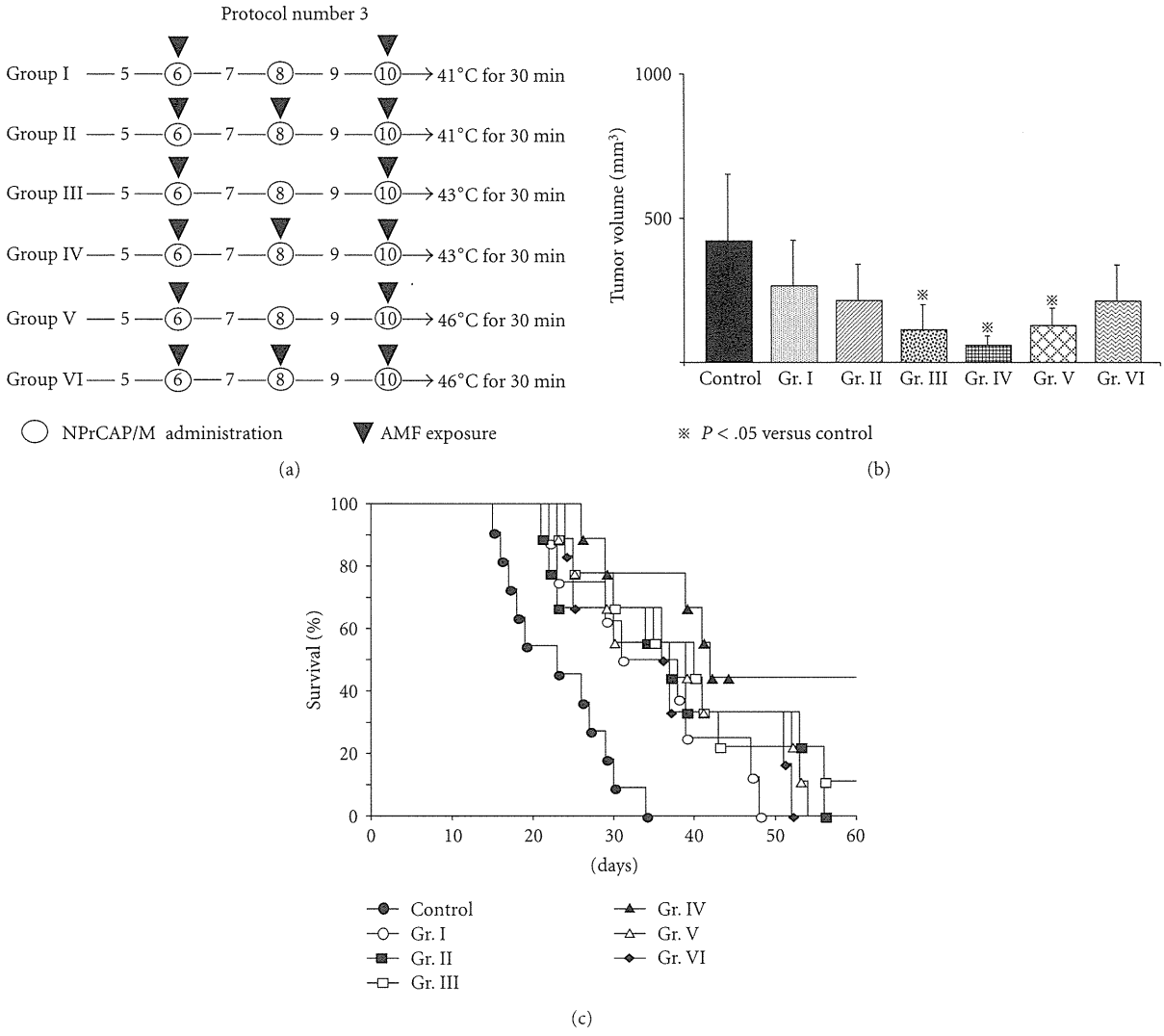

FIGURE 5: Time schedules and results for tumor volume, survival periods and rates of mice treated by Protocol number 3. (a) Protocols of Groups I, II, III, IV, V, and VI. (b) Tumor volumes on day 14 after re-challenge with B16F1 melanoma. All data are presented as mean ± standard deviation. Tumor volumes of Groups III, IV, and V were significantly reduced compared with the control group ($P = .0045, .0004$, and .0085 resp.) by the Scheffé test. (c) Kaplan-Meier survival curve over a period of 60 days after tumor re-challenge. Survival rates of Groups III and IV were significantly prolonged compared with that of the control group ($P = .0011$ and .0002, resp.). One of the nine mice in Group III and four of the nine mice in Group IV were protected against re-challenge with B16F1 melanoma cells.

two cell lines, the majority of subsequent studies listed in Protocols number 1 through number 4 were conducted on B16F1 cells.

3.3. Effective Growth Inhibition of B16F1 Melanoma Cells at the Site of Re-Challenge, Second Transplantation by NPrCAP/M with AMF Exposure (Protocol number 1). We then evaluated whether NPrCAP/M treatment with or without heat in the local primary tumor could inhibit the growth of distant tumors which were not given an intratumor injection of NPrCAP/M. There was a significant difference in the melanoma growth inhibition of re-challenge transplants between the groups of NPrCAP/M with and without heat. NPrCAP/M with AMF exposure showed the most significant growth inhibition in re-challenge melanoma and increased life span of the host animals, that is, 30%–50% complete growth inhibition (rejection) of re-challenge melanoma growth, indicating that NPrCAP/M with heat possesses a thermo-immunotherapeutic effect. For this, we treated the primary B16F1 and F10 melanoma cells by NPrCAP/M and then measured the volume of the secondary melanoma after the second transplantation at a different site to the first transplant. We also evaluated the survival periods

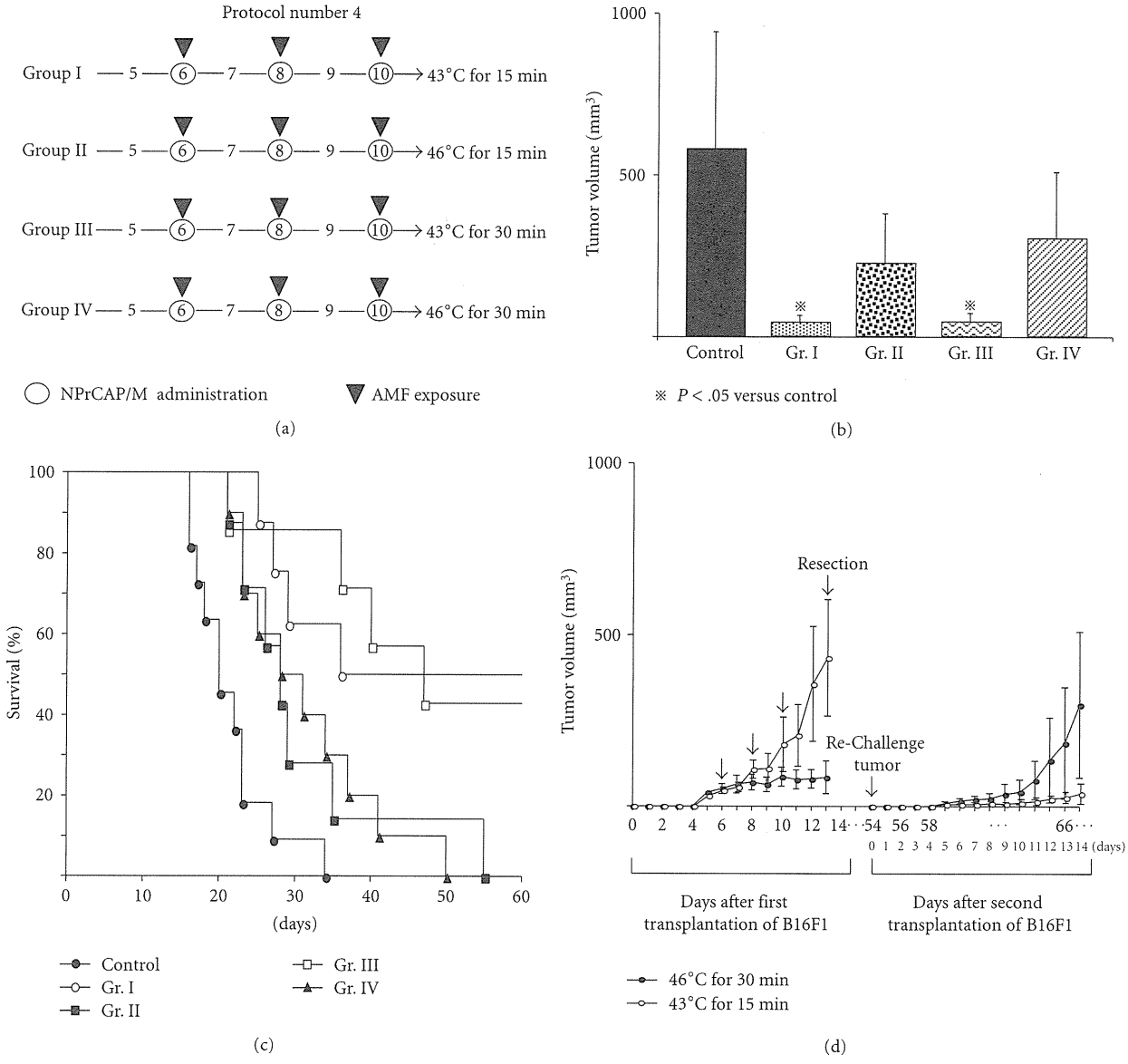

FIGURE 6: Time schedules and results for tumor volumes, survival periods, and rates for treatment with Protocol number 4. (a) Protocols of Groups I, II, III, and IV. (b) Tumor volumes on day 14 after re-challenge with B16F1 cells. All data are presented as mean ± standard deviation. Tumor volumes of Groups I and III on day 14 were significantly reduced compared with that of the control group ($P = .0009$ and .0016, resp.) by Scheffé test. (c) Kaplan-Meier survival curve over a period of 60 days after re-challenge. Survival rates of Group I and III were significantly prolonged compared with that of the control group ($P = .0004$ and .0005, resp.). Four of the eight mice in Group I and three of the seven mice in Group III were protected against re-challenge with B16F1 melanoma cells. (d) Tumor volumes of the primary tumor and re-challenge tumor as representative examples of Groups I ($n = 8$) and IV ($n = 10$) which were treated at 43°C for 15 minutes and 46°C for 30 minutes, respectively. All data are presented as mean ± standard deviation.

and rates of host melanoma-bearing mice. These secondary melanomas were not directly exposed to NPrCAP/M; hence we could evaluate the thermo-immunotherapeutic effect of NPrCAP/M treatment.

First, we compared the therapeutic effects among Groups I (intratumor injection of magnetite nanoparticles alone without AMF exposure), II (magnetite injection and heat at 43°C for 30 minutes by AMF), III (NPrCAP/M injection without AMF), and IV (NPrCAP/M injection and heat at 43°C for 30 minutes by AMF) of Protocol number 1 (Figure 3(a)). As shown in Figure 3(b), NPrCAP/M-mediated hyperthermia at 43°C showed the most significant

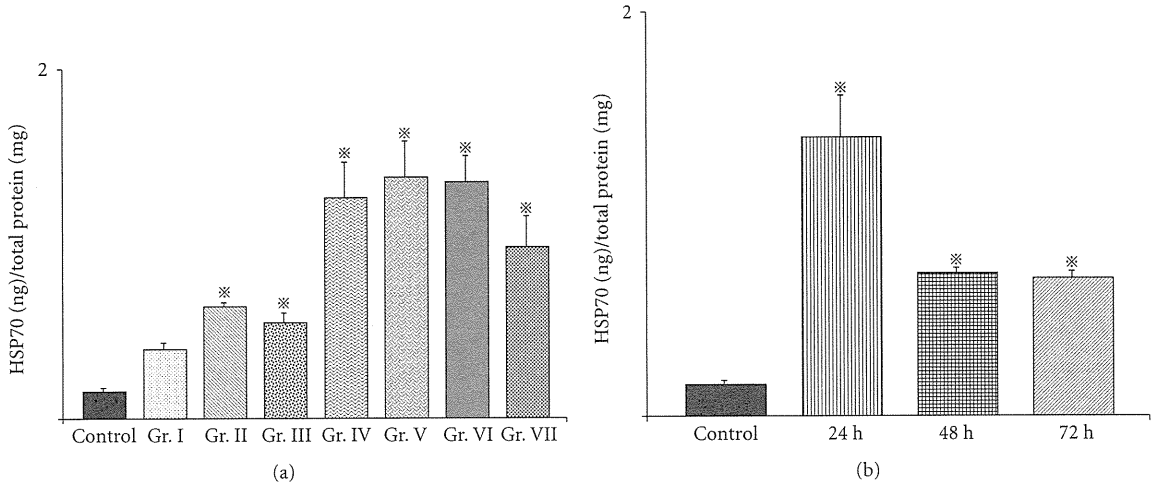

FIGURE 7: Expression of HSP70 in a tumor after thermotherapy. (a) Amounts of HSP70 in tumors 24 hours after thermotherapy as described in the Materials and Methods. All data are presented as mean ± standard deviation ($n = 4$). There were significant differences between the control group and all other groups except Group I by Dunnett's test ($P < .05$). (b) Amounts of HSP70 24, 48, and 72 hours after thermotherapy at 43°C for 30 minutes. All data are presented as mean ± standard deviation ($n = 4$). There were significant differences between the control group and all other groups by Dunnett's test ($P < .05$).

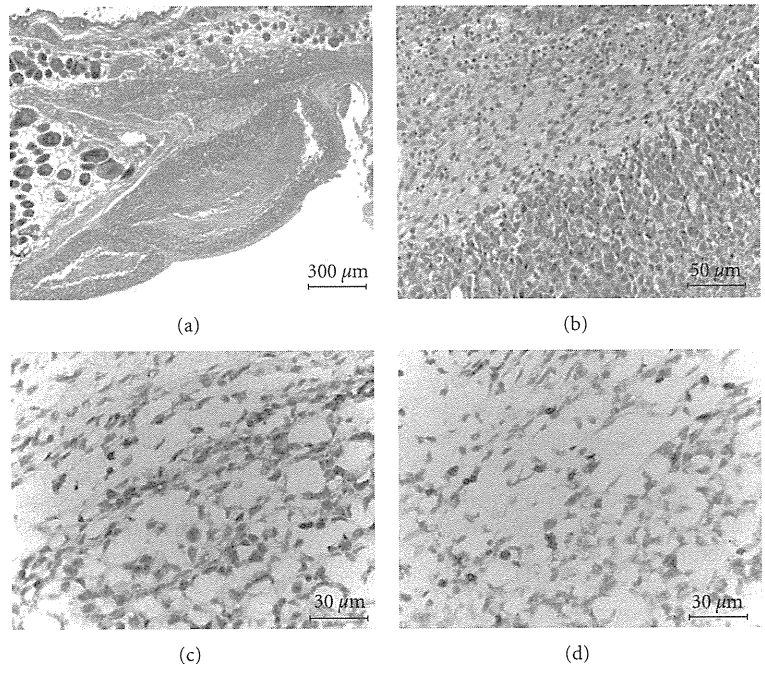

FIGURE 8: Histopathology and immunohistochemistry of a re-challenge tumor. (a) A low-power view of a re-challenge tumor with HE staining (×49). (b) A high-power view (×200). Monocytic infiltrates are seen around a necrotic lesion. (c) $CD4^+$ T cells (×400). (d) $CD8^+$T cells (×400). Almost equal numbers of $CD4^+$ and $CD8^+$ T cells are observed.

growth inhibition of secondary B16F1 melanoma in re-challenged mice. Both magnetite nanoparticles with heat at 43°C and NPrCAP/M without heat also inhibited the growth of secondary melanomas, though statistically not significant (Figure 3(b) and (c)). Most importantly, NPrCAP/M alone without heat caused equal growth inhibition of secondary melanomas to that induced by magnetite with AMF exposure, suggesting some immunotherapeutic effect of NPrCAP/M. A similar growth inhibition of secondary transplanted melanoma cells was obtained in B16F10 (Figure 2).

Next, we compared the life span of the host animals among 4 groups. The survival of mice in Group IV was prolonged, compared with that of the control group (P = .0003) and Group I (P = .0003). Three of the ten mice in Group IV (30%) were protected completely from re-challenge with B16F1 cells (Figure 3(c)). Magnetite alone with AMF exposure at 43°C (Group II) and NPrCAP/M alone without heat (Group III) failed to show any statistically significant prolongation of the host animal survival.

3.4. Effect of Treatment Frequency for the Primary Tumor on Growth Inhibition of Re-Challenge Melanoma (Protocol number 2). To evaluate the effect of the number of treatments for the primary tumor on the re-challenge tumor, six treatment approaches were designed using B16F1 cells. They consisted of hyperthermia once on day 6 (Group I), twice on days 6 and 8 (Group II) or days 6 and 10 (Group III), three times on days 6, 8, and 10 (Group IV) or 6, 7, and 8 (Group V), and a total of five times on days 6 through 10 (Group VI) (Figure 4(a)). Melanoma tumor volumes in re-challenged mice were smallest in Groups III and IV, while the longest survival periods and rates were obtained in Group IV with complete growth inhibition (rejection) of second re-challenge being 33% (n = 9) on day 60 (Figures 4(b) and 4(c)). The consecutive irradiation on days 6, 7, and 8 (Group V) or days 6 through 10 resulted in larger volumes of secondary tumors and poorer survival periods and rates compared to Group III or IV (Figures 4(b) and 4(c)). These findings suggested that repeated hyperthermia, once a day every other day for a total of three days, could induce effective degradation of B16 melanoma cells, which then most likely induced host immunity against melanoma.

3.5. Effect of Temperature and Treatment Frequency on Melanoma Growth Inhibition in Re-Challenge Mice (Protocol number 3). Our study indicated that the most effective thermo-immunotherapy for re-challenge B16 melanoma can be obtained at a temperature of 43°C for 30 minutes with the treatment repeated three times on every other day intervals without complete degradation of the primary melanoma. We compared growth inhibition of secondly transplanted melanomas at therapeutic temperatures of 41°C, 43°C, and 46°C for 30 minutes twice on days 6 and 10, or three times on days 6, 8, and 10 (Figure 5(a)). As shown in Figures 5(b) and 5(c), thermotherapy at 43°C in Group IV (43°C, every other day for a total of three times on three days) was the most effective for the growth inhibition of both the secondly transplanted, re-challenge melanoma and for improving the survival rates and duration of host mice. Four of the nine mice in Group IV (44.4%) were protected completely against re-challenge with B16F1 melanoma on day 60 (Figure 5(c)).

Our therapeutic conditions and their effects differ from those of magnetically mediated hyperthermia on the transplanted melanomas reported previously [29]. MCL-mediated hyperthermia for B16 melanoma showed that hyperthermia at 46°C once or twice led to regression of 40%–90% of primary tumors and to 30%–60% survival of mice, whereas hyperthermia at 43°C failed to induce regression of the secondary tumors with 0% survival of mice [29].

3.6. Effect of Temperature and Treatment Duration on Melanoma Growth Inhibition in Re-Challenge Mice (Protocol number 4). We then compared the effects of temperature and duration of NPrCAP/M-mediated hyperthermia at 43°C for 15 minutes, 43°C for 30 minutes, 46°C for 15 minutes, and 46°C for 30 minutes on the re-challenge with B16F1 melanoma (Figure 6(a)). Tumor volumes and survival rates and periods of treatment of mice clearly showed that hyperthermia at 43°C elicited a more significant effect than that at 46°C (Figures 6(b) and 6(c)). Four of the eight mice (50%) in Group I (43°C for 15 minutes) and three of the seven mice (42.8%) in Group III (43°C for 30 minutes) survived 60 days after a second transplantation of B16F1 (Figure 6(c)), suggesting that NPrCAP/M with heat to the primary melanoma at 43°C for 15–30 minutes inhibits significantly the growth of distant metastatic melanoma, complete growth inhibition (rejection) of the second re-challenge melanoma being 42%–50%. Hyperthermia at 46°C for 30 minutes strongly inhibited the growth of the B16F1 tumor but had little effect on the re-challenge tumor, whereas hyperthermia at 43°C for 15 minutes hardly inhibited the growth of the primary tumor but strongly inhibited that of the second re-challenge tumor (Figure 6(d)). These findings suggest that NPrCAP/M-mediated hyperthermia at 43°C can be used most effectively to treat distant metastatic melanoma.

3.7. Production of HSP70 by NPrCAP/M Treatment and Presence of $CD8^+$ T Cells around and within the Re-Challenge Melanoma. Heat shock protein forms a complex with intracellular peptides released from degrading tumor cells and presented by the MHC class I molecules of professional antigen-presenting cells [23]. We analyzed HSP70 production in the primary tumor and $CD4^+$ and $CD8^+$ T cell infiltration into the re-challenge secondary tumor. Figure 7(a) shows the amounts of HSP70 in the tumors at 24 hours after the NPrCAP/M-mediated hyperthermia. Among the six treatment groups, conditions of hyperthermia at 43°C for 15 or 30 minutes and 46°C for 15 minutes were equally effective for induction of HSP70 as those at 41°C for 15 minutes or 30 minutes and at 46°C for 30 minutes (Figure 7(a)). We also investigated whether expression of HSP70 in the posttherapeutic tumors depended on the duration of AMF exposure (15 minutes or 30 minutes), heating temperature (41°C, 43°C, or 46°C), and time elapsed after exposure (24 hours, 48 hours, or 72 hours). Figure 7(b) shows that the amount of HSP70 in the treated B16F1 tumors was most abundant at 24 hours after hyperthermia at 43°C, and over-expression of HSP70 was maintained at a significant level after 72 hours. Although thermotherapy at 46°C for 15 minutes could induce HSP70 as abundantly as that at 43°C for 30 minutes (Figure 7(a)), this condition failed to suppress the re-challenge melanoma transplant as

efficiently as 43°C thermotherapy (Figures 5(b) and 5(c)). This suggests that immunological factors other than HSPs are at least in part responsible for growth inhibition and rejection of the re-challenge melanoma. Hyperthermia at 43°C for 1 hour mediated the expression of MHC class I molecules after 24 hours in association with enhanced expression of HSP70 [30]. Heat treatment of tumor cells permits enhanced cross-priming, possibly via up-regulation of both HSPs and tumor antigen expression [24]. By inducing HSP70 and possibly MHC class I, immune T cells could aggregate around melanoma cells. We thus examined histochemically the immunological reaction against secondly transplanted, re-challenge B16F1 melanoma in hematoxylin and eosin (HE)- and CD4- and CD8-stained sections. In addition to neutrophilic leukocytes, macrophages, and plasma cells, $CD4^+$ and $CD8^+$ T cells were observed around and within the re-challenge tumors with necrotic lesions (Figures 8(a), 8(b), 8(c), and 8(d)). These T cells were seen with a small number around the first transplant melanoma treated by NPrCAP/M with or without AMF exposure but hardly observed around the naive B16F1 tumors in mice that were not treated by NPrCAP/M-mediated thermotherapy (data not shown). This may indicate that melanoma-specific T cell immunity is likely involved in our NPrCAP/M therapy strategy.

4. Conclusions

This study has provided the basis for developing a melanoma targeted chemo-immuno-thermotherapy (CTI) strategy by conjugating melanogenesis substrate, NPrCAP with magnetite nanoparticles after exposure to alternating magnetic field. NPrCAP/M-mediated hyperthermia at a relatively low temperature (43°C) effectively inhibited the growth of second transplant, re-challenge melanoma. Possibly, superficially bound NPrCAP possesses important roles in targeting nanoparticles to melanocytic cells and a chemotherapeutic effect on these cells. Based upon the present animal therapeutic protocol, that is, three-every-other-day treatment at 43°C, we have started preliminary clinical trials (phase I/II) of NPrCAP/M CTI therapy with a significant success to a limited number of advanced stages III and IV melanoma patients. Four patients entered in this trial after approval of the Ethics Committee of Sapporo Medical University and two of them showed PR and CR, still surviving and carrying out normal daily life for more than 24 months [31].

Lastly, it should be noted that melanin intermediates produce reactive oxygen species such as superoxide and H_2O_2 [4, 32, 33]. This unique biological property of melanin intermediates not only causes cell death but also may produce immunogenic properties. In fact, NPrCAP/M alone without heat was as effective as magnetite nanoparticles with AMF exposure in inhibiting growth of re-challenge melanoma (Figures 3(b) and 3(c)). It would be interesting to know whether the growth of secondary re-challenge melanoma could be inhibited after treatment of NPrCAP alone onto the primary tumor [34]. The molecular background of our NPrCAP/M CTI therapy needs to be further studied.

Acknowledgments

The authors thank Toda Kogyo Co. (Hiroshima, Japan) and Meito Sangyo Co., Ltd. (Nagoya, Japan) for supplying magnetite nanoparticles and technical advice for the synthesis of NPrCAP/M, respectively. This work was supported by a Health and Labor Sciences Research Grant-in-Aid for Research on Advanced Medical Technology from the Ministry of Health, Labor and Welfare of Japan (H21-Nano-006). they wish to express their appreciation to Ms. Masae Okura for the technical help in conducting this research.

References

[1] K. Jimbow, T. Iwashina, F. Alena, K. Yamada, J. Pankovich, and T. Umemura, "Exploitation of pigment biosynthesis pathway as a selective chemotherapeutic approach for malignant melanoma," *The Journal of Investigative Dermatology*, vol. 100, supplement 2, pp. 231S–238S, 1993.

[2] F. Alena, T. Iwashina, A. Gili, and K. Jimbow, "Selective in vivo accumulation of N-acetyl-4-S-cysteaminylphenol in B16F10 murine melanoma and enhancement of its in vitro and in vivo antimelanoma effect by combination of buthionine sulfoximine," *Cancer Research*, vol. 54, no. 10, pp. 2661–2666, 1994.

[3] J. M. Pankovich and K. Jimbow, "Tyrosine transport in a human melanoma cell line as a basis for selective transport of cytotoxic analogues," *Biochemical Journal*, vol. 280, no. 3, pp. 721–725, 1991.

[4] K. Reszka and K. Jimbow, "Electron donor and acceptor properties of melanin pigments in the skin," in *Oxidative Stress in Dermatology*, J. Fuchs and L. Packer, Eds., pp. 287–320, Marcel Dekker, New York, NY, USA, 1993.

[5] M. Tandon, P. D. Thomas, M. Shokravi, et al., "Synthesis and antitumour effect of the melanogenesis-based antimelanoma agent N-Propionyl-4-S-cysteaminylphenol," *Biochemical Pharmacology*, vol. 55, no. 12, pp. 2023–2029, 1998.

[6] P. D. Thomas, H. Kishi, H. Cao, et al., "Selective incorporation and specific cytocidal effect as the cellular basis for the antimelanoma action of sulphur containing tyrosine analogs," *The Journal of Investigative Dermatology*, vol. 113, no. 6, pp. 928–934, 1999.

[7] O. Algan, H. Fosmire, K. Hynynen, et al., "External beam radiotherapy and hyperthermia in the treatment of patients with locally advanced prostate carcinoma," *Cancer*, vol. 89, no. 2, pp. 399–403, 2000.

[8] M. D. Hurwitz, I. D. Kaplan, J. L. Hansen, et al., "Association of rectal toxicity with thermal dose parameters in treatment of locally advanced prostate cancer with radiation and hyperthermia," *International Journal of Radiation Oncology, Biology, Physics*, vol. 53, no. 4, pp. 913–918, 2002.

[9] M. Johannsen, U. Gneveckow, L. Eckelt, et al., "Clinical hyperthermia of prostate cancer using magnetic nanoparticles: presentation of a new interstitial technique," *International Journal of Hyperthermia*, vol. 21, no. 7, pp. 637–647, 2005.

[10] N. Kawai, A. Ito, Y. Nakahara, et al., "Anticancer effect of hyperthermia on prostate cancer mediated by magnetite cationic liposomes and immune-response induction in transplanted syngeneic rats," *Prostate*, vol. 64, no. 4, pp. 373–381, 2005.

[11] S. Lindquist, "The heat-shock response," *Annual Review of Biochemistry*, vol. 55, pp. 1151–1191, 1986.

[12] A. Konno, N. Sato, A. Yagihashi, et al., "Heat- or stress-inducible transformation-associated cell surface antigen on the activated H-ras oncogene-transfected rat fibroblast," *Cancer Research*, vol. 49, no. 23, pp. 6578–6582, 1989.

[13] A. Ménoret and R. Chandawarkar, "Heat-shock protein-based anticancer immunotherapy: an idea whose time has come," *Seminars in Oncology*, vol. 25, no. 6, pp. 654–660, 1998.

[14] P. K. Srivastava, A. Ménoret, S. Basu, R. Binder, and K. Quade, "Heat shock proteins come of age: primitive functions acquired new roles in an adaptive world," *Immunity*, vol. 8, no. 6, pp. 657–665, 1998.

[15] Y. Tamura, N. Tsuboi, N. Sato, and K. Kikuchi, "70 kDa heat shock cognate protein is a transformation-associated antigen and a possible target for the host's anti-tumor immunity," *The Journal of Immunology*, vol. 151, no. 10, pp. 5516–5524, 1993.

[16] Y. Tamura, P. Peng, K. Liu, M. Daou, and P. K. Srivastava, "Immunotherapy of tumors with autologous tumor-derived heat shock protein preparations," *Science*, vol. 278, no. 5335, pp. 117–120, 1997.

[17] D. D. Mosser, A. W. Caron, L. Bourget, C. Denis-Larose, and B. Massie, "Role of the human heat shock protein hsp70 in protection against stress-induced apoptosis," *Molecular and Cellular Biology*, vol. 17, no. 9, pp. 5317–5327, 1997.

[18] Y. Tamura and N. Sato, "Heat shock proteins: chaperoning of innate and adaptive immunities," *Japanese Journal of Hyperthermic Oncology*, vol. 19, pp. 131–139, 2003.

[19] P. K. Srivastava, "Immunotherapy for human cancer using heat shock protein-peptide complexes," *Current Oncology Reports*, vol. 7, no. 2, pp. 104–108, 2005.

[20] S. Takashima, N. Sato, A. Kishi, et al., "Involvement of peptide antigens in the cytotoxicity between 70-kDa heat shock cognate protein-like molecule and $CD3^+$, $CD4^-$, $CD8^-$, TCR-$\alpha\beta$- killer T cells," *The Journal of Immunology*, vol. 157, no. 8, pp. 3391–3395, 1996.

[21] M. Yanase, M. Shinkai, H. Honda, T. Wakabayashi, J. Yoshida, and T. Kobayashi, "Antitumor immunity induction by intracellular hyperthermia using magnetite cationic liposomes," *Japanese Journal of Cancer Research*, vol. 89, no. 7, pp. 775–782, 1998.

[22] G. Ueda, Y. Tamura, I. Hirai, et al., "Tumor-derived heat shock protein 70-pulsed dendritic cells elicit-tumor-specific cytotoxic T lymphocytes (CTLs) and tumor immunity," *Cancer Science*, vol. 95, no. 3, pp. 248–253, 2004.

[23] A. Ito, H. Honda, and T. Kobayashi, "Cancer immunotherapy based on intracellular hyperthermia using magnetite nanoparticles: a novel concept of "heat-controlled necrosis" with heat shock protein expression," *Cancer Immunology, Immunotherapy*, vol. 55, no. 3, pp. 320–328, 2006.

[24] H. Shi, T. Cao, J. E. Connolly, et al., "Hyperthermia enhances CTL cross-priming," *The Journal of Immunology*, vol. 176, no. 4, pp. 2134–2141, 2006.

[25] A. Ito, M. Fujioka, T. Yoshida, et al., "4-S-cysteaminylphenol-loaded magnetite cationic liposomes for combination therapy of hyperthermia with chemotherapy against malignant melanoma," *Cancer Science*, vol. 98, no. 3, pp. 424–430, 2007.

[26] M. Sato, T. Yamashita, M. Ohkura, et al., "N-propionyl-cysteaminylphenol-magnetite conjugate (NPrCAP/M) is a nanoparticle for the targeted growth suppression of melanoma cells," *The Journal of Investigative Dermatology*, vol. 129, no. 9, pp. 2233–2241, 2009.

[27] A. A. Brozyna, L. VanMiddlesworth, and A. T. Slominski, "Inhibition of melanogenesis as a radiation sensitizer for melanoma therapy," *International Journal of Cancer*, vol. 123, no. 6, pp. 1448–1456, 2008.

[28] A. Slominski, B. Zbytek, and R. Slominski, "Inhibitors of melanogenesis increase toxicity of cyclophosphamide and lymphocytes against melanoma cells," *International Journal of Cancer*, vol. 124, no. 6, pp. 1470–1477, 2009.

[29] M. Suzuki, M. Shinkai, H. Honda, and T. Kobayashi, "Anticancer effect and immune induction by hyperthermia of malignant melanoma using magnetite cationic liposomes," *Melanoma Research*, vol. 13, no. 2, pp. 129–135, 2003.

[30] A. Ito, M. Shinkai, H. Honda, T. Wakabayashi, J. Yoshida, and T. Kobayashi, "Augmentation of MHC class I antigen presentation via heat shock protein expression by hyperthermia," *Cancer Immunology, Immunotherapy*, vol. 50, no. 10, pp. 515–522, 2001.

[31] K. Jimbow, T. Takada, M. Sato, et al., "Melanin biology and translational research strategy; melanogenesis and nanomedicine as the basis for melanoma-targeted DDS and chemothermo-immunotherapy," *Pigment Cell and Melanoma Research*, vol. 21, no. 2, p. 243, 2008.

[32] K. Jimbow, Y. Miyake, K. Homma, et al., "Characterization of melanogenesis and morphogenesis of melanosomes by physicochemical properties of melanin and melanosomes in malignant melanoma," *Cancer Research*, vol. 44, no. 3, pp. 1128–1134, 1984.

[33] Y. Minamitsuji, K. Toyofuku, S. Sugiyama, and K. Jimbow, "Sulphur containing tyrosinase analogs can cause selective melanocytoxicity involving tyrosinase-mediated apoptosis," *The Journal of Investigative Dermatology*, vol. 4, no. 2, pp. 130S–136S, 1999.

[34] Y. Osai, M. Ohkura, Y. Tamura, et al., "Intratumoral administration of melanoma targeting N-propionyl cysteaminylphenol induces in vivo anti-melanoma effect and tumor specific immunity," *Pigment Cell & Melanoma Research*, vol. 21, no. 2, p. 329, 2008.

Pigment Cell Melanoma Res. **22**; 623–634

ORIGINAL ARTICLE

Agouti protein, mahogunin, and attractin in pheomelanogenesis and melanoblast-like alteration of melanocytes: a cAMP-independent pathway

Tokimasa Hida[1,2], Kazumasa Wakamatsu[3], Elena V. Sviderskaya[1], Andrew J. Donkin[1], Lluis Montoliu[4], M. Lynn Lamoreux[5], Bin Yu[6], Glenn L. Millhauser[6], Shosuke Ito[3], Gregory S. Barsh[7], Kowichi Jimbow[2] and Dorothy C. Bennett[1]

1 Division of Basic Medical Sciences, St. George's, University of London, Cranmer Terrace, London, UK **2** Department of Dermatology, Sapporo Medical University, Sapporo, Hokkaido, Japan **3** Department of Chemistry, Fujita Health University School of Health, Sciences, Toyoake, Aichi, Japan **4** Department of Molecular and Cellular Biology, Centro Nacional de Biotecnología (CNB-CSIC), Campus de Cantoblanco, and Centro de Investigación Biomédica en Red de Enfermedades Raras (CIBERER), ISCIII, Madrid, Spain **5** Comparative Genetics Program, Texas A&M University, College Station, TX, USA **6** Department of Chemistry and Biochemistry, University of California, Santa Cruz, CA, USA **7** Howard Hughes Medical Institute and the Department of Pediatrics and Genetics, Stanford University Medical Center, Stanford, CA, USA

CORRESPONDENCE D. C. Bennett, e-mail: dbennett@sgul.ac.uk

KEYWORDS pheomelanin/agouti/Mc1r/cAMP/melanoblast/attractin/mahogunin

PUBLICATION DATA Received 10 October 2008, revised and accepted for publication 15 May 2009

doi: 10.1111/j.1755-148X.2009.00582.x

Summary

Melanocortin-1 receptor (MC1R) and its ligands, α-melanocyte stimulating hormone (αMSH) and agouti signaling protein (ASIP), regulate switching between eumelanin and pheomelanin synthesis in melanocytes. Here we investigated biological effects and signaling pathways of ASIP. Melan-a non agouti (*a/a*) mouse melanocytes produce mainly eumelanin, but ASIP combined with phenylthiourea and extra cysteine could induce over 200-fold increases in the pheomelanin to eumelanin ratio, and a tan-yellow color in pelletted cells. Moreover, ASIP-treated cells showed reduced proliferation and a melanoblast-like appearance, seen also in melanocyte lines from yellow (*A^y/a* and *$Mc1r^e/Mc1r^e$*) mice. However ASIP-YY, a C-terminal fragment of ASIP, induced neither biological nor pigmentary changes. As, like ASIP, ASIP-YY inhibited the cAMP rise induced by αMSH analog NDP-MSH, and reduced cAMP level without added MSH, the morphological changes and depigmentation seemed independent of cAMP signaling. Melanocytes genetically null for ASIP mediators attractin or mahogunin (*$Atrn^{mg\text{-}3J/mg\text{-}3J}$* or *$Mgrn1^{md\text{-}nc/md\text{-}nc}$*) also responded to both ASIP and ASIP-YY in cAMP level, while only ASIP altered their proliferation and (in part) shape. Thus, ASIP–MC1R signaling includes a cAMP-independent pathway through attractin and mahogunin, while the known cAMP-dependent component requires neither attractin nor mahogunin.

Significance

Many animal colors and patterns as well as human hair and eye color are genetically determined through the relative amounts of eumelanin and pheomelanin synthesized. Humans with red (pheomelanic) hair in general, and with specific hypomorphic *MC1R* mutations in particular, have increased susceptibility to melanoma, and the mechanism for this remains uncertain. Melanin, especially pheomelanin, has been implicated in mutagenesis in melanocytes by ultraviolet light, particularly UVA, via release of reactive oxygen species that can damage DNA. Ability to regulate the switch between eumelanin and pheomelanin synthesis in cultured melanocytes would greatly aid studies of mutagenesis and photocarcinogenesis in these cells. This work may also shed some light on the longstanding puzzle of how cAMP levels and ASIP can control both melanocytic differentiation and pigment-type switching.

Introduction

The diverse patterns of mammalian coat color are determined by the quantity and distribution of just two types of organic pigment: eumelanin (black to brown) and pheomelanin (yellow to red) (Barsh, 2006; Ito, 2003). Both are produced by melanocytes in the hair bulbs and basal epidermis. They are synthesized and accumulate in melanosomes, specialized organelles which are transferred to keratinocytes of the hair and epidermis (Jimbow et al., 2000). Each melanocyte can produce either eumelanin or pheomelanin, depending on the hormonal and chemical environment (Barsh, 2006). In agouti (wild-type) mice the dorsal hairs are black with a sub-apical yellow band because, in the hair cycle, follicular melanocytes produce first eumelanin, then pheomelanin, then eumelanin again (pigment-type switching) (Barsh, 2006).

Genetic studies of coat color in mice have contributed greatly to our understanding of the mechanisms of melanin synthesis and its regulation (Bennett and Lamoreux, 2003). Two major loci are central to pigment-type switching in mouse. One is the agouti locus encoding agouti signal protein (ASIP), with mutants including non agouti (*a*, giving a eumelanic black mouse in the absence of other mutations) and dominant yellow (A^y); the other is the melanocortin-1 receptor (*Mc1r*) locus, formerly extension (*e*), also with both eumelanic and pheomelanic mutants (e.g. recessive yellow, $Mc1r^e$) (Barsh, 2006). Melanocortin-1 receptor (MC1R) is a cell-surface G-protein-coupled receptor for which the best-known agonist is the soluble peptide αMSH, cleaved from the precursor pro-opiomelanocortin (POMC) in the pituitary and skin (Barsh, 2006; García-Borrón et al., 2005). Binding of αMSH to MC1R is known to activate adenylate cyclase and cAMP synthesis, promoting eumelanin synthesis through both post-translational [review: (Bennett, 1989)] and transcriptional pathways via microphthalmia-related transcription factor (MITF) (Bertolotto et al., 1998; Levy et al., 2006). Microphthalmia-related transcription factor is a master regulator for eumelanogenesis, melanocyte differentiation, proliferation, and survival. It promotes transcription of melanocyte-specific gene products including melanosomal enzymes tyrosinase, TYRP1 and DCT and the matrix protein SILV/PMEL (Levy et al., 2006). Synthesis of both eumelanin and pheomelanin starts from tyrosine oxidation catalyzed by tyrosinase (Ito, 2003). The resulting dopaquinone can be a precursor for either eumelanin synthesis, promoted by TYRP1 and DCT, or pheomelanin in the presence of high cysteine concentrations and/or low tyrosinase activity (Ito, 2003; Land et al., 2003).

Agouti signaling protein is a soluble protein of 131 amino acids, apparently secreted by dermal papilla cells in hair bulbs. It competitively antagonizes αMSH at the MC1R and inhibits the eumelanogenic signal, downregulating melanogenic enzymes and leading to pheomelanin synthesis (Barsh, 2006; Millar et al., 1995).

The above account does not however explain certain data on pigment-type switching. Firstly, a homozygous null mutation of *Pomc* has no effect on the black pigmentation of *a/a* mice (Slominski et al., 2005), and has also been reported in a black-haired human (Clément et al., 2008) consistent with reports that MC1R has constitutive activity (Barsh, 2006; García-Borrón et al., 2005; Sanchez-Mas et al., 2004). While ASIP requires the MC1R to affect melanocytes, it can signal in the absence of added αMSH (Abdel-Malek et al., 2001; Sakai et al., 1997; Sviderskaya et al., 2001), thus acting as an inverse agonist at the MC1R rather than just an MSH antagonist (Barsh, 2006). Secondly, molecules outside the cAMP pathway are indispensable for ASIP to signal pheomelanogenesis. Mice with null mutations at the attractin (*Atrn,* formerly mahogany) or mahogunin (*Mgrn1,* formerly mahoganoid) loci produce eumelanin and no pheomelanin, even in the presence of ASIP (He et al., 2001, 2003). Attractin is a type I transmembrane protein proposed to be an obligatory accessory receptor for ASIP, while MGRN1 is an E3 ubiquitin ligase (Barsh, 2006). Although their precise contributions to ASIP signaling remain unclear, ATRN and MGRN1 are components with ASIP and MC1R of a conserved biochemical and genetic pathway (He et al., 2003). Thirdly, ASIP has not been found to enhance pheomelanogenesis in cultured melanocytes, although ASIP can inhibit cAMP generation in MC1R-expressing cells including melanocytes (Abdel-Malek et al., 2001; Le Pape et al., 2008; Ollmann et al., 1998). No culture conditions have been developed in which melanocytes produce exclusively pheomelanin, even with ASIP. This suggests that either a factor(s) present in vivo is missing, or that something present in cultures may prevent pheomelanogenesis.

To aid understanding of ASIP signaling, we have sought to develop culture conditions under which ASIP contributes to overt pheomelanin synthesis by the melan-a immortal murine melanocyte line. We report conditions enabling substantially increased pheomelanin/eumelanin ratios and visibly yellow cell pellets. To elucidate ASIP signaling, we also established new mouse melanocyte lines of four relevant mutant genotypes, namely A^y mutant cells from mice with constitutive ASIP synthesis from a housekeeping promoter, $Mc1r^e/Mc1r^e$ cells with a non-functional MC1R receptor, and melanocytes with null mutations of *Atrn* and *Mgrn1*. Taken together, the data demonstrate that ASIP signaling can reduce melanocyte growth and induce morphological dedifferentiation as well as affecting pigmentation. These biological effects are mimicked in genetically yellow melanocytes without added ASIP, are incomplete in *Atrn*- and *Mgrn1*-null melanocytes, appear

independent of cAMP downregulation, and require the amino terminus of ASIP.

Results

Melanoblast-like morphology and reduced proliferation of melanocytes grown with ASIP

Melan-a cells (*a/a*) grown with 12-*O*-tetradecanoyl phorbol-13-acetate (TPA) normally show a dendritic, well-differentiated appearance with abundant eumelanosomes (Figure 1) (Bennett et al., 1987). The appearance of these cells was dramatically changed however within 5 days' culture with 10 nM murine ASIP. The cells became shorter, smaller, and less dendritic, often with a crescent shape and ruffled membrane on the convex side, and markedly less pigmented (Figure 1). This appearance resembled that of normal and immortal melanoblasts – unpigmented melanocyte precursors – in similar media (Figure 1; Sviderskaya et al., 1995). Melanoblasts are the predominant growing population in primary neonatal epidermal cultures in our melanocyte medium in the first 7–10 days, after which they differentiate into melanocytes (Sviderskaya et al., 1995). Agouti signaling protein was apparently inducing rapid morphological dedifferentiation of melan-a cells, although a few cells (possibly non-dividing) remained well-pigmented. Transitional forms were rare (Figure 1). The proliferation rate of melan-a cells was also significantly reduced in the presence of ASIP (data in a later section), as also reported by Le Pape et al. (2008).

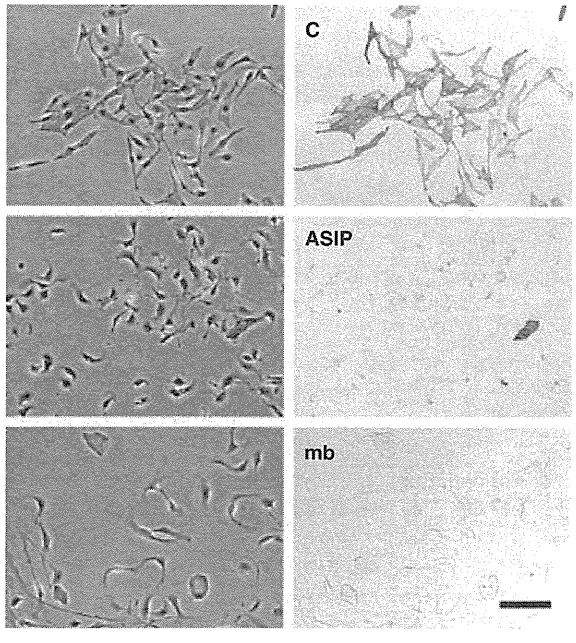

Figure 1. Morphological and pigmentary changes induced in melan-a cells by agouti signaling protein (ASIP). Paired phase contrast (left) and bright-field (right, to show eumelanin) images of melan-a cells grown in normal growth medium (C, control); or in the same medium with 10 nM ASIP added for the last 5 days (ASIP). No phenylthiourea (PTU) or extra cysteine was present (see text). (mb): normal murine melanoblasts in a primary neonatal epidermal melanocyte culture, 7 days after explantation, showing similarity to melan-a cells grown with ASIP. Bar = 100 μm.

To assess the specificity of these morphological changes, the effect of ASIP was tested on melan-e2 melanocytes, derived from *Mc1r*^{e}/ *Mc1r*^{e} mice lacking the normal MC1R. Agouti signaling protein had no detectable effect on these cells, indicating that the morphological effect is specific (details in a later section).

Pheomelanin/eumelanin ratio markedly enhanced by ASIP, cysteine, and PTU

Pheomelanin and eumelanin content and their ratio in melan-a cells were quantitated by chemical degradation and high performance liquid chromatography. In preliminary experiments, no increase of pheomelanin content was detected on growth with ASIP alone, as previously reported by others. Therefore other relevant factors, the cysteine concentration and tyrosinase activity [using the tyrosinase inhibitor phenylthiourea (PTU)], were modulated together with ASIP addition. Cells were preincubated with PTU for 2 weeks beforehand to allow dilution of preexisting eumelanin by cell proliferation (melan-a cells in the absence of keratinocytes do not significantly secrete or degrade melanin, as recently confirmed by Le Pape et al. (2008)), and monitoring only of melanin synthesized during the experiment. In a typical experiment, eumelanin content was reduced around 10-fold after growth with 10 nM ASIP for 14 days, while pheomelanin content was not affected (Figure 2). The pheomelanin/eumelanin ratio was thus increased over 10-fold. In the presence of ASIP, an additional 2 mM cysteine reduced eumelanin content further, and increased pheomelanin content, while continuation of PTU addition (100 μM) substantially reduced eumelanin content without significantly affecting pheomelanin (Figure 2). With ASIP, cysteine, and PTU together pheomelanin content was around four times that with ASIP alone. In the experiment shown, the pheomelanin and eumelanin ratio in cells grown with ASIP, cysteine, and PTU was 0.13, over 200-fold higher than with no addition, and strikingly high compared with other findings with cultured melanocytes. Cell pellets were brown rather than black in color (not shown). In a separate experiment, melan-a cell pellets were prepared after culture with and without combinations of these factors and TPA (TPA was previously present throughout). Here cells were precultured with 500 μM rather than 300 μM PTU to assist complete depletion of eumelanin, and grown with ASIP etc for 5 days only. The combination of ASIP and high cysteine now gave a tan-yellow cell pellet, or white with continued PTU addition (Figure 2B). Overlap of the exposure to high PTU with ASIP treatment would have prevented the synthesis of any eumelanin in the period before ASIP had taken effect, but

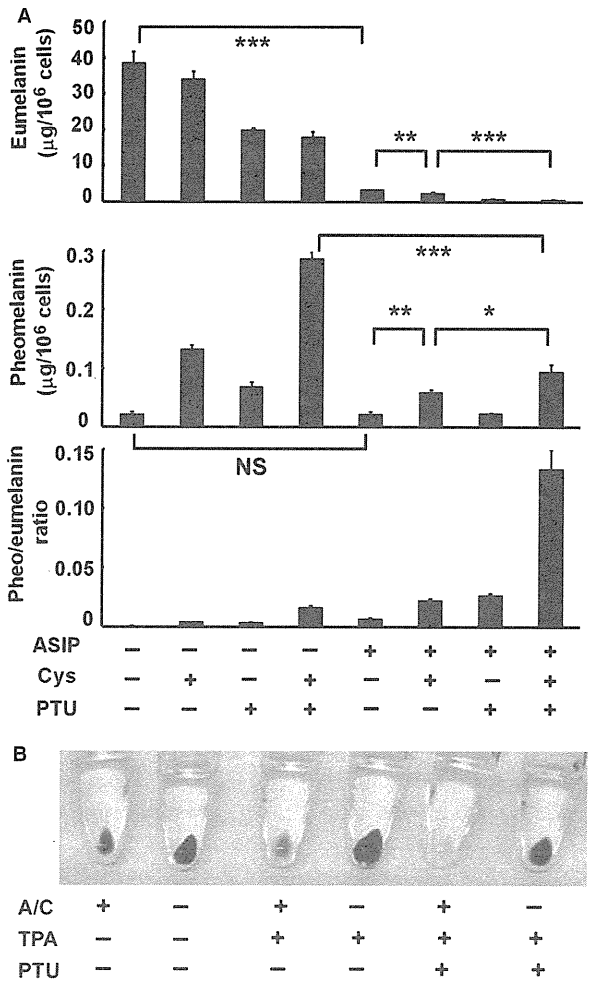

Figure 2. Marked increases in pheomelanin/eumelanin ratio and tan coloration by agouti signaling protein (ASIP), cysteine and phenylthiourea (PTU). Cells were subcultured as needed to prevent confluency. (A) Eumelanin and pheomelanin content of melan-a cells after 14 days' growth with 300 μM PTU followed by 14 days' growth in standard medium [containing 12-*O*-tetradecanoyl phorbol-13-acetate (TPA)] with the indicated additives. Data show mean ± SEM of three different samples. (ASIP): 10 nM ASIP; (Cys): 2 mM cysteine plus 100 μM mercaptoethanol; (PTU): 100 μM PTU. (B) Pellets of cells after 14 days' growth with 500 μM PTU followed by 5 days' growth with the indicated additives. (A/C): 10 nM ASIP, 2 mM cysteine and 100 μM mercaptoethanol; (TPA): 200 nM TPA; (PTU): PTU at 500 μM for 2 days and 100 μM for 3 days. Significances of selected differences by Student's *t*-test (two-tailed) are shown: *$P < 0.05$; **$P < 0.01$; ***$P < 0.001$, (NS): $P > 0.05$, not significant.

reduction of the PTU level was then necessary for any melanin synthesis at all to occur. Supplementation of the precursor cysteine was evidently needed for synthesis of enough pheomelanin to give a yellow color. Pellets of cells grown without TPA were darker than those with TPA, and smaller, reflecting lower cell numbers (slower growth).

Melanocytes from lethal yellow and recessive yellow mice: ASIP-like effects on cell morphology and growth

For comparison with the effects of ASIP and as further potential pheomelanic melanocytes, we established three independent immortal melanocyte lines from each of two genotypes of yellow mice, by crossing an *Ink4a-Arf* knockout allele into the strain to prevent cell senescence (Sviderskaya et al., 2002). Lines melan-Ay1 to -3 were grown from A^y/a mice, in which ASIP is expressed ubiquitously from a housekeeping promoter, including in melanocytes, through a genomic rearrangement (Duhl et al., 1994). Lines melan-e1 to -e3 were obtained from recessive yellow ($Mc1r^e/Mc1r^e$) mice, which express a truncated, non-functional MC1R (Robbins et al., 1993). The yellow hair in both genotypes contains almost exclusively pheomelanin by HPLC analysis (Ozeki et al., 1995).

All lines derived were from *Ink4a-Arf*$^{-/-}$ mice. Melanocytes of both yellow genotypes were difficult to grow, with sparse plating and slow growth in all cultures compared with other genotypes in our experience. Initially the cells were maintained in standard conditions with TPA and cholera toxin (CT, 200 pM) to promote proliferation. Cultures of a given genotype appeared similar. The three melan-e cultures appeared hypersensitive to 200 pM CT, with high dendricity, pigmentation and reduced growth; accordingly CT was varied and stocks were grown with 20 pM CT (which appeared optimal) for a number of passages. Cells in all lines of both genotypes now appeared similar: dark, well-differentiated, large, flat, bipolar or polygonal cells, usually with numerous visible melanosomes, and similar to melan-a cells with 20 pM CT (Figure 3). The cell color by light microscopy and the pellet color (not shown) were black. For further studies a single line of each type was used, melan-Ay1 and melan-e2. Cholera toxin was removed entirely from both lines after passage 10. Growth seemed to be transiently inhibited, then recovered. Both melan-Ay and melan-e cells without CT became small, curly and bipolar, with few dendrites and little pigment, again resembling melanoblasts (Figure 3, compare Figure 1). Melan-Ay cells grew more slowly in growth medium alone than with 20 pM CT or 100 pM NDP-MSH [(4-Nle, 7-D-Phe)-α-melanocyte stimulating hormone, a serum-stable synthetic MSH analog] (doubling times 2.6, 1.6 and 1.5 days respectively, averaged over three passages with duplicate dishes). Likewise, melan-e cells showed doubling times of 2.1 and 1.4 days without and with 20 pM CT. Like melan-a cells with ASIP, some melan-Ay and melan-e cells without CT remained heavily pigmented and dendritic. The change was reversible in both melan-Ay and melan-e cells: when reincubated with CT, they regained the previous melanocytic appearance (melan-e: Figure S1; not shown for melan-Ay).

Melan-e cells responded to very low CT concentrations, becoming pigmented and dendritic with as little as

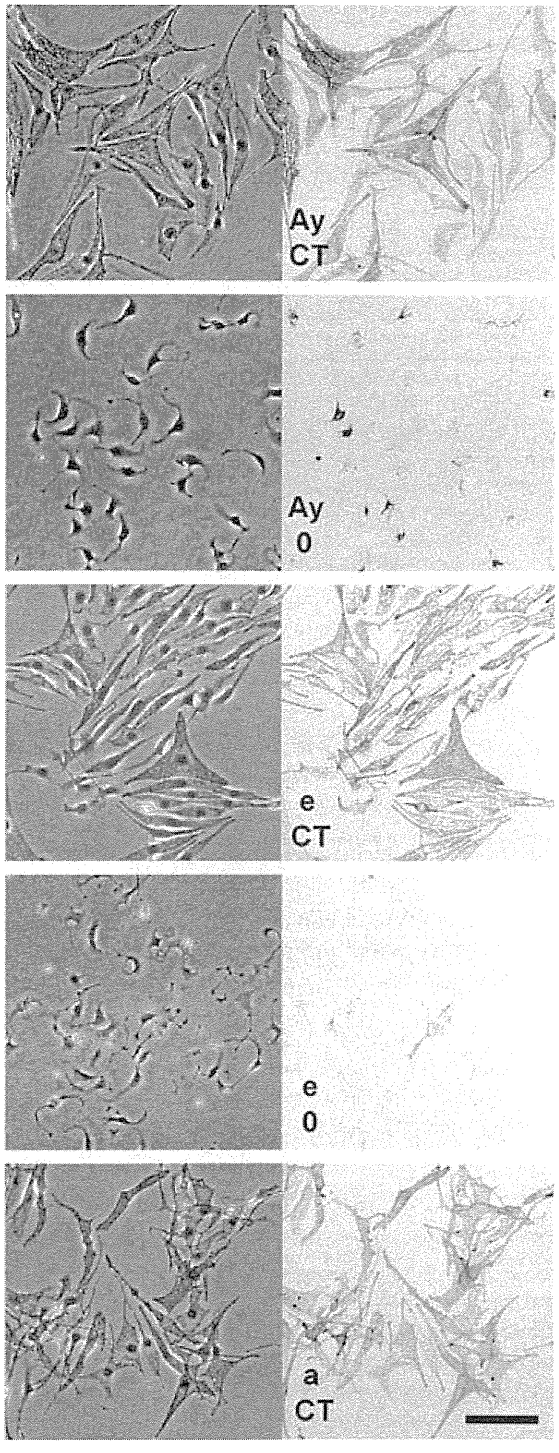

Figure 3. Melanoblast-like appearance of melan-Ay and melan-e cells in the absence of CT. Paired phase-contrast (left) and bright-field (right) images of melan-Ay (Ay) and melan-e (e) cells grown with 20 pM CT (CT) or for several passages without CT (0). Some residual eumelanin is seen in some cells of both genotypes without CT. For reference melan-a cells (a) grown with 20 pM CT are also shown; there is little difference from melan-a cells without CT (Figure 1). Bar = 100 μm.

300 fM CT (Figure S1). These conditions were now utilized to test the specificity of the morphological effects of ASIP. Melan-e cells were grown with or without CT (300 fM) and with or without ASIP (10 nM). Agouti signaling protein had no detectable effect on melan-e cells under either set of conditions (Figure S1). Conversely, melan-a cells with 300 fM CT did respond to ASIP by switching to melanoblast-like morphology as usual (Figure S1), confirming that 10 nM ASIP can counteract 300 fM CT in MC1R-positive cells. Together, these findings show that the induction of melanoblast-like morphology by ASIP is receptor-mediated and specific.

A carboxy-terminal fragment of ASIP: lack of effect on cell number, shape or pigmentation of melan-a cells

To analyze ASIP signaling further, the ASIP C-terminal analog ASIP-YY was tested. ASIP-YY corresponds to the cysteine-rich domain, ASIP(80–132), with residues 115 and 124 mutated to tyrosine (Y) to improve protein folding (McNulty et al., 2005). This domain of ASIP is sufficient for high-affinity receptor binding in vitro. ASIP-YY displaces NDP-MSH from human melanocortin receptors expressed on HEK-293 human kidney cells, and inhibits αMSH-stimulated cAMP production, demonstrating competitive antagonism (McNulty et al., 2005).

Unexpectedly, melan-a cells grown with up to 100 nM ASIP-YY showed no visible difference from control cells (Figure 4A), and no effect on melanin content nor cell growth, although 10 nM ASIP induced the usual shape-change and depigmentation in parallel cultures (Figure 4B, C). To ensure that our ASIP-YY preparation retained its known inhibitory activity, we evaluated its inhibition of MSH-induced cAMP production in melan-a cells. Cells were stimulated with 30 pM NDP-MSH (found to give maximal stimulation in this assay – data not shown), and intracellular cAMP was quantitated by ELISA. NDP-MSH alone induced a more than 200-fold increase in cAMP concentration (Figure 5A, black bars). Neither 1 nM ASIP nor 1 nM ASIP-YY affected this increase, but 10 nM and 100 nM ASIP reduced it by 2/3 and to zero respectively (Figure 5A, striped bars). ASIP-YY did inhibit the cAMP stimulation to a similar extent (Figure 5A, dotted bars). To exclude the possibility that ASIP-YY is rapidly degraded in serum-containing medium, 100 nM ASIP or 100 nM ASIP-YY were incubated with culture medium containing 10% fetal bovine serum (FBS) at 37°C overnight and the mixture was used as stimulating buffer for cAMP measurements. Both ASIP and ASIP-YY still inhibited the MSH-induced cAMP rise completely (Figure 5A, bars with asterisks). Thus, ASIP-YY could inhibit cAMP stimulation as effectively as ASIP. Lastly, as seen in Figure 5C, melanocytes cultured in the absence of added melanocortin showed similar decreases in cAMP level with either ASIP or ASIP-YY. This excluded the possibility that the biological effects were mediated only through an

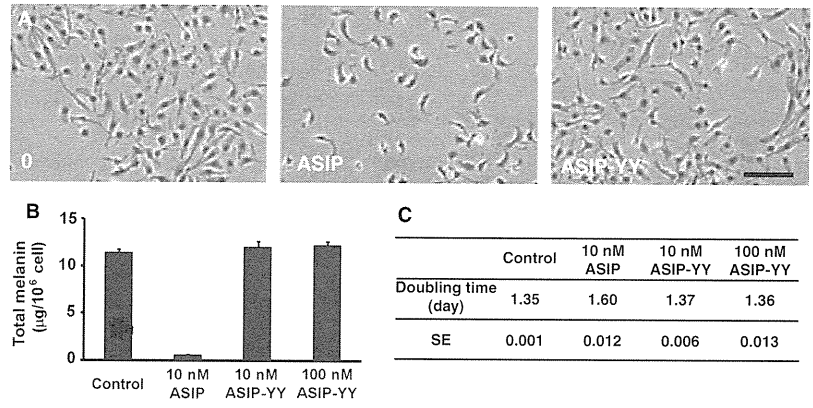

C

	Control	10 nM ASIP	10 nM ASIP-YY	100 nM ASIP-YY
Doubling time (day)	1.35	1.60	1.37	1.36
SE	0.001	0.012	0.006	0.013

Figure 4. Melanoblast-like shape-change, depigmentation and growth inhibition of melan-a cells by agouti signaling protein (ASIP) but not ASIP-YY. (A) phase-contrast images of melan-a cells grown for 5 days in growth medium (0), with 10 nM ASIP (ASIP) or with 100 nM ASIP-YY (ASIP-YY). Bar = 100 μm. (B) Total melanin content of melan-a cells grown in growth medium only, or with ASIP or ASIP-YY for 14 days. Mean and SEM of triplicate dishes. (C) Cell doubling times of melan-a cells subcultured with no addition, ASIP or ASIP-YY for 30 days. Shown are mean ± SEM of triplicates.

inverse agonist effect of ASIP upon cAMP level, with the effect not being shared by ASIP-YY.

Atrn and *Mgrn1*-null melanocytes: partial biological responses to ASIP but not ASIP-YY

To investigate molecular requirements for the ASIP effects, immortal melanocytes were isolated carrying the null mutations $Atrn^{mg\text{-}3J}$ (melan-mg1 and -2) and $Mgrn1^{md\text{-}nc}$ (melan-md1 and -2). Attractin specifically binds the amino-terminal domain of ASIP, apparently behaving as an accessory receptor for ASIP. $Atrn^{mg\text{-}3J}$ homozygotes are completely resistant to ASIP hair-color effects in vivo (He et al., 2001). The intracellular E3 ubiquitin ligase mahogunin (MGRN1) also seems crucial: $Mgrn1^{md\text{-}nc}$ homozygous mice likewise lack any pigmentary response to ASIP (He et al., 2003).

These cultures were from *Ink4a-Arf*$^{+/-}$ animals. Again, lines of the same genotype appeared indistinguishable and are not specified here. Growth from both mutant genotypes was initially very slow, attributable to *Ink4a-Arf* hemizygosity, but lines were eventually established. Lines melan-mg2 and -md1 were used for more detailed studies. Both lines retained slower growth than melan-a cells (Figure 6), but this was comparable to growth of the non-mutant cultures from littermate *Ink4a-Arf* heterozygous mice of the same strains: melan-a6 (md control) and melan-a7 (mg control) showed doubling times of 2.4+/−0.10 and 1.9+/−0.17 days (mean, SEM) respectively. Hence this slow growth was not due to the pigmentary genotype. Melan-mg cells grown without CT had a well-differentiated, flat appearance with numerous black melanosomes (Figure 6, Figure S2). After growth with 10 nM ASIP, they showed a partial response: a somewhat melanoblast-like appearance with variable reduction or clustering of melanosomes (Figure S2), and markedly slower growth, but 10 nM ASIP-YY gave no detectable change in shape or growth rate (Figure 6). Melan-md cells displayed a highly differentiated melanocytic appearance with long, branching dendrites and heavy pigmentation in normal medium without CT (Figure 6, Figure S2). On growth with 10 nM ASIP, there was only a subtle shape change, with shorter and less-branched dendrites, a slight crescentic appearance and cells remaining visibly black-pigmented. However, proliferation was significantly reduced, whereas 10 nM ASIP-YY affected neither morphology nor proliferation (Figure 6).

Inhibition of MSH-induced cAMP rise by both ASIP and ASIP-YY in melan-mg and melan-md cells

cAMP was assayed in melan-mg and melan-md cells and control melan-a cells after stimulation by NDP-MSH with or without ASIP or ASIP-YY (Figure 5B). Interestingly, both 100 nM ASIP and 100 nM ASIP-YY completely inhibited the MSH-induced cAMP rise in both genotypes, implying that this inhibition requires neither ATRN nor MGRN1.

Discussion

Here we show that recombinant ASIP induces morphological dedifferentiation of cultured melanocytes to a melanoblast-like shape (reduced cell size and dendricity, acquired crescent shape) and retards growth, as well as strongly inhibiting eumelanogenesis and greatly increasing the pheomelanin to eumelanin ratio, especially in the presence of extra cysteine and PTU. The promotion of pheomelanogenesis by PTU is consistent with the biochemical kinetics favoring cysteinyldopa formation at low tyrosinase activity (Ito and Wakamatsu, 2008). The inhibition of melanogenesis and proliferation by ASIP in melan-a cells were also recently reported by Le Pape et al. (2008), but genetic requirements, receptor-specificity and cysteine effects were not analyzed. There

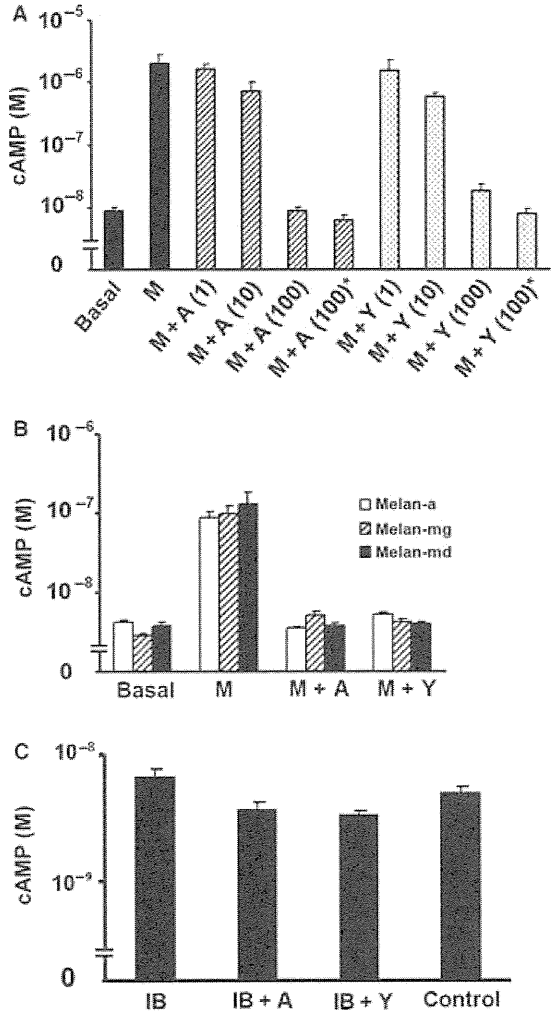

Figure 5. (A) Inhibition of NDP-MSH-induced cAMP rise by both agouti signaling protein (ASIP) and ASIP-YY in melan-a cells. Intracellular cAMP per well was measured in cultures that had been plated and allowed to attach overnight, after stimulation for 30 min with 30 pM NDP-MSH (M), with or without ASIP (A) or ASIP-YY (Y). Figures in parentheses are concentration of ASIP or ASIP-YY in nM. *RPMI1640 medium with 10% FBS was incubated with ASIP or ASIP-YY at 37°C overnight and was used as stimulating buffer, followed by application of NDP-MSH. Shown are mean ± SEM of triplicate wells. (B) Inhibition of NDP-MSH-induced cAMP rise by both ASIP and ASIP-YY in melan-mg and melan-md cells. Assay as above, using 100 nM ASIP (A) or 100 nM ASIP-YY (Y). The reason for the lower apparent stimulation of melan-a cells by NDP-MSH in (B) than in (A) is unknown; it may reflect change in the assay reagents with time. However the relative responses of different genotypes are clear. (C) Reduction of basal cAMP by both ASIP and ASIP-YY. In this experiment only, to increase assay sensitivity, melan-a cells were plated at a higher number of 6×10^4 cells/well, preincubation with isobutylmethylxanthine (IBMX) was for 5 h at 1 μM, and incubation with the stated additives was for 5 h. IBMX alone (1 μM, a low concentration) had no significant effect, whereas both ASIP (A) and ASIP-YY (Y) at 10 nM gave significant reductions in cAMP levels compared with 1 μM IBMX alone ($P = 0.013$, $P = 0.003$ respectively). Similar effects were seen under slightly varied conditions (not shown).

were some minor differences in outcomes, for example they saw a reduction in pheomelanin content with ASIP alone and we did not; these may be attributable to differences in protocol (for example our longer treatment times), in exact culture conditions or in cell passage level. Le Pape et al. (2009) have also now reported a valuable microarray analysis of gene expression changes in melan-a cells grown with ASIP, which supports the concept of partial dedifferentiation and complements the present findings; for example reduced expression of a large number of pigmentary genes including *Mitf* was noted after growth with ASIP.

Several observations in the present study indicate that the morphological dedifferentiation seen with ASIP is a specific effect rather than due to a contaminant. Firstly, the cell shape change was deficient in MGRN1-null melan-md cells and ATRN-null melan-mg cells, and completely absent from MC1R-null melan-e cells grown with a trace of CT. Secondly, the altered cells looked like normal melanoblasts rather than appearing abnormal or unhealthy. We have never observed any other substance to transform melan-a cells in this way; on the other hand ASIP does inhibit forward differentiation of melanoblasts (Aberdam et al., 1998; Sviderskaya et al., 2001). Thirdly, the same melanoblast-like shape was also observed in melan-Ay cells without CT (and without added ASIP), indicating that it could also be induced by endogenous mouse ASIP. Again it was seen in melan-e melanocytes without CT, and it was suppressed in both melan-Ay and melan-e cells by CT.

Surprisingly, these morphological changes and reduced melanin content were not provoked by the ASIP C-terminus (ASIP-YY), although this fully inhibited the stimulation of cAMP by MSH, and reduced the cAMP level in the absence of added melanocortin. Thus, reduced intracellular cAMP is not sufficient for any of the biological effects of ASIP observed here, even though many findings support the sufficiency of increased cAMP for forward melanocytic differentiation [reviews: (Bennett, 1989; Bertolotto et al., 1998)], including the effects reported here of CT, a cAMP agonist.

The growth inhibition by ASIP apparently also required the *N*-terminus of ASIP, as it was not produced by ASIP-YY. However it required neither MGRN1 nor ATRN, as melan-md and -mg cells were also inhibited, if anything more markedly than melan-a cells. This was the only tested biological effect of ASIP not diminished in melan-mg and -md cells. Surprisingly, it appeared independent of the ability to reduce cAMP level, as ASIP-YY affected cAMP but not growth. We cannot entirely discount the possibility that this growth inhibition was partly non-specific, but a counterargument is that slower growth than in wild-type melanocytes also accompanied the melanoblast-like phenotype seen in melan-Ay cells which make endogenous ASIP, and melan-e cells without CT.

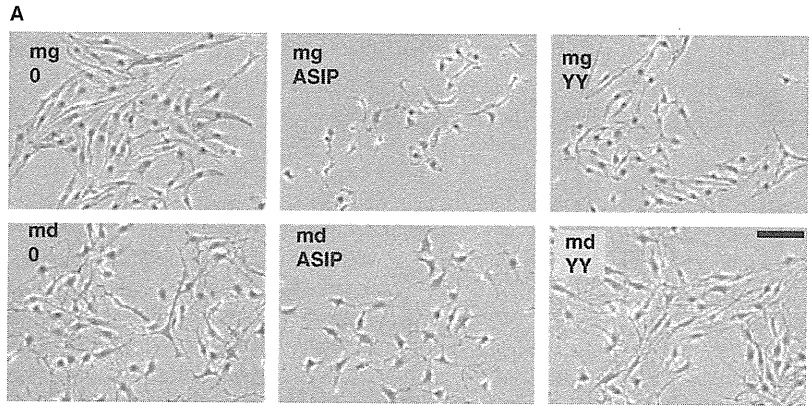

B

Melan-mg

	Control	10 nM ASIP	10 nM ASIP-YY
Doubling time (day)	1.88	4.77	1.84
SE	0.012	0.134	0.005

C

Melan-md

	Control	10 nM ASIP	10 nM ASIP-YY
Doubling time (day)	2.54	4.38	2.60
SE	0.054	0.206	0.034

Figure 6. Melanoblastic shape-change and growth inhibition of melan-mg and melan-md cells by agouti signaling protein (ASIP) but not ASIP-YY. Melan-mg cells (mg) and melan-md cells (md) were incubated for 5 days in growth medium alone (0), with 10 nM ASIP (ASIP) or with 10 nM ASIP-YY (YY). Bar = 100 μm. No Cys or phenylthiourea (PTU) present. Cell doubling times of melan-mg cells (B) and melan-md cells (C) were measured in the presence of 10 nM ASIP or 10 nM ASIP-YY for 30 days. Shown are mean ± SEM of triplicate cultures. Retardation of proliferation by ASIP was highly significant for both genotypes by Student's *t*-test ($P < 0.001$), while ASIP-YY had no significant effect.

Melanocortin receptors and ATRN are the only molecules known to bind ASIP (Abdel-Malek et al., 2001; He et al., 2003). Attractin is required for ASIP effects in the mouse, and was suggested to function to enhance ASIP–MC1R binding (Barsh, 2006). Thus it was surprising that we saw partial morphological and depigmentation effects of ASIP on ATRN-null melanocytes. Perhaps ASIP also has some partial effects in vivo in ATRN-null mice, but they are not sufficient to dilute visibly the black color of hair. Agouti signaling protein (ASIP)'s morphological effects were very deficient in MGRN1-null melanocytes, consistent with the requirement of MGRN1 for ASIP action in mice.

Through which signaling pathway does ASIP/MC1R induce biological effects, if not through reduced cAMP? Each of five melanocortin receptor subtypes couples to adenylate cyclase, generating cAMP and activating PKA (García-Borrón et al., 2005). Other signaling intermediates reported to be activated by MSH/MC1R in melanocytes or melanoma cells include protein kinase C, nitric oxide, p38MAPK and p42/p44MAPK, with the first three reported to stimulate melanogenesis/differentiation, but in each case there was evidence that the effect was dependent on cAMP signaling (Buffey et al., 1992; Englaro et al., 1995; Park et al., 2006; Smalley and Eisen, 2000; Tsatmali et al., 2000). Another candidate pathway is through G_q and/or phospholipase C. Coupling to inositol triphosphate (IP_3) and Ca^{2+}signaling (which G_q and phospholipase C could mediate) has been reported for a number of human and mouse melanocortin receptors, including MC1R (Eves et al., 2003; García-Borrón et al., 2005; Mountjoy et al., 2001). Recently, a novel high-affinity ligand for MC1R was identified in dogs, namely canine β-defensin 103 (CBD103), encoded at the *K* locus (Candille et al., 2007). Transgenic mice expressing cDNAs for either of two (canine) CBD103 alleles on an *A/A* (agouti) background had a black coat color. Canine and human β-defensins could bind dog, mouse and human MC1Rs, but not ASIP-YY. Interestingly, neither canine cDNA affected cAMP concentration in melan-a melanocytes. CBD103 might act by competitively inhibiting ASIP binding, or might elicit cAMP-independent signaling from the MC1R to promote eumelanogenesis (Candille et al., 2007).

Considering this with our results, we hypothesize dual signaling from MC1R, as follows (Figure 7). Melanocortin-1 receptor can activate both cAMP and another signaling pathway X. Activation of X may be cAMP-dependent or -independent; X may also be the cAMP-independent pathway activated by β-defensins. Agouti signaling protein can antagonize cAMP signaling through its *C*-terminus (as in ASIP-YY) and independently antagonize X signaling through its *N*-terminus and through ATRN and MGRN1, resulting in inhibition of eumelanogenesis, enhancement of pheomelanogenesis (under suitable conditions), and melanoblast-like morphology. To explain the activation of eumelanogenesis by cAMP, yet persistence of eumelanogenesis when the cAMP signal is withdrawn, we suggest a positive feedback loop (Figure 7), likely to involve MITF as MITF mediates melanocytic differentiation. Agouti signaling protein can also downregulate MITF gene expression

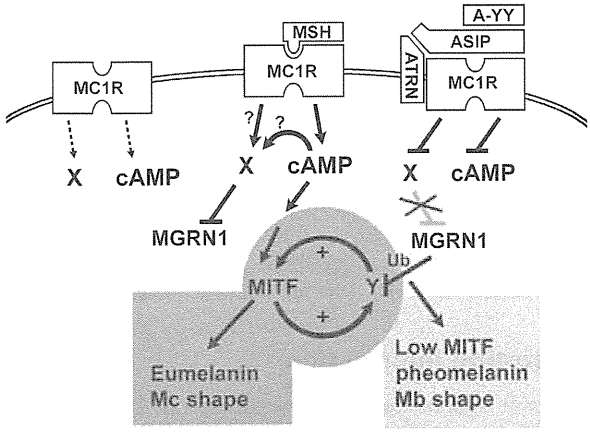

Figure 7. Model to account for responsiveness to cAMP level in activation but not inactivation of eumelanin synthesis. See Discussion for main explanation. (A-YY) ASIP-YY, (Mc) melanocyte, (Mb) melanoblast, (Ub) ubiquitinylation. Melanocortin-1 receptor (MC1R) is shown with some basal activity (left, lost in *e* mutant), to explain why POMC null, *a/a* mice are black, and related data (see text). (This might alternatively be due to BD103 or some unknown signal). Agouti signaling protein (ASIP) would not be required for pheomelanogenesis unless Y has been switched on by the MC1R/cAMP pathway, hence inactive MC1R would give a yellow color even with deficient MGRN1, as seen in *e/e, md/md* mice.

(Le Pape et al., 2009). The components of this proposed loop remain to be elucidated, but we suggest that MGRN1, a ubiquitin ligase, may break the loop by ubiquitinating and destabilizing one component Y. This would lead to a less-differentiated state with low MITF activity, permissive for pheomelanogenesis.

Full pigment type-switching to give predominantly pheomelanin and a clear yellow color has not been achieved in cultured melanocytes or melanoma cells treated with ASIP (Graham et al., 1997; Sakai et al., 1997), or ASIP and PTU (Le Pape et al., 2008). Likewise, pheomelanin content in melan-a cells was not increased by ASIP alone in this study. With ASIP, cysteine and PTU however, a substantially increased pheomelanin/eumelanin ratio of 0.13 was seen here, although this was not complete pigment type-switching, as the ratio in yellow mouse hair can exceed 100:1 (Ozeki et al., 1995). Moreover, visibly yellow pelletted cells were obtained with a specific combination of intensive PTU pretreatment, ASIP and cysteine, illustrating the sensitivity of the pheomelanin–eumelanin ratio to precise culture history. Further work is needed to produce overt pigment-type switching in culture, but further combinations of the above factors may prove fruitful.

Receptor-specific induction of a melanoblast-like shape from melanocytes by ASIP and a similar effect of MC1R inactivity have not been reported before. The recurrent melanoblast-like morphology in genetically yellow and ASIP-treated melanocytes suggests a possible relationship between dedifferentiation and pheomelanogenesis, supported by the known inhibition of forward melanoblast differentiation by ASIP. *Mc1r^{e}/Mc1r^{e}* melanocyte cultures were reported previously, but were grown with dibutyryl cAMP and were described only as pigmented (Costin et al., 2004). Melan-a cells treated with ASIP lose expression of TYRP1, DCT, and SILV/PMEL, all needed to generate normal eumelanosomes but not pheomelanosomes, while retaining low tyrosinase expression (Sakai et al., 1997) which would favor pheomelanogenesis (Ito, 2003). Thus a partial equivalence between melanoblasts and the cells that make pheomelanin seems possible; melanoblasts do express some tyrosinase (Sviderskaya et al., 1995), have low DCT, TYRP1, and MITF (Aberdam et al., 1998), and contain premelanosomes (Hirobe and Takeuchi, 1978). Premelanosomes and pheomelanosomes are evidently not the same, as the latter contain pheomelanin, but the difference may depend on relatively minor factors such as cysteine concentration.

Taken together, our results indicate that ASIP's biological effects require a cAMP-independent signaling pathway via MC1R and MGRN1 and facilitated by ATRN, which plays a key role in regulating melanogenesis and melanocyte morphology.

Materials and methods

Reagents

Tissue culture plastics and FBS were from Gibco Europe (Paisley, UK). Cholera toxin, TPA, PTU (also known as phenylthiocarbamide), NDP-MSH and 3-isobutyl-1-methylxanthine (IBMX) were from Sigma Chemical Co. (Poole, UK). Full length recombinant mouse ASIP was generated using a baculovirus expression system; material used for these studies was purified by cation and anion exchange chromatography as previously described (Ollmann et al., 1998), and was >99% pure. ASIP-YY was synthesized as described (McNulty et al., 2005), was 90–95% pure and has MC1R binding activity equivalent to that of normal ASIP (McNulty et al., 2005). All protein factor stock solutions were prepared in Dulbecco's phosphate-buffered saline (PBS) lacking $CaCl_2$ and $MgCl_2$, with bovine serum albumin (1 mg/ml) as carrier, and stored at −70°C. For all experiments involving cysteine addition to culture medium, 100 μM mercaptoethanol was added to enhance cysteine stability.

Establishment of immortal murine melanocyte lines

Mice were of the C57BL/6J inbred strain and *a/a* at the agouti/*A-SIP* locus unless otherwise stated. All experiments complied with local and European legislation concerning vivisection and the experimentation and use of animals for research purposes. Mice with color mutations were crossed to mice carrying an *Ink4a-Arf* deletion allele for one or more generations, to give *Ink4a-Arf*$^{-/-}$ or $^{+/-}$ offspring that yield diploid melanocytes deficient in cell senescence and readily established in culture (Sviderskaya et al., 2002). For melan-Ay-1 to -3, *A^{y}/a, Ink4a-Arf*$^{-/-}$ mice were generated from *A^{y}/a* mice kindly provided by FR Gruijl, Leiden University Medical Center, the Netherlands. A dermal fibroblast line of this genotype, fibro-Ay, was also isolated as a potential source of secreted ASIP; not characterized further. For melan-e1 to -e3, *Mc1r$^{e/e}$, Ink4a-Arf*$^{-/-}$ mice were used. For melan-mg1 and -mg2 (*Atrn* null) and

melan-md1 and -md2 (*Mgrn1* null), *Atrn*$^{mg\text{-}3J/mg\text{-}3J}$, *Ink4a-Arf* $^{+/-}$ mice on a C3H *a/a* background and *Mgrn1*$^{md\text{-}nc/md\text{-}nc}$, *Ink4a-Arf* $^{+/-}$ mice on a mixed *a/a* strain background were generated (inbred not available). Neonatal mouse skins were sent to London in chilled culture medium, and used to isolate epidermal melanocytes with the aid of immortal keratinocyte feeder cells as described (Sviderskaya et al., 1997, 2002), using RPMI1640 medium (Sigma) containing 10% FBS, 200 nM TPA, and 200 pM CT, gassed with CO_2 (10% v/v). Routine subculture was as described (Sviderskaya et al., 1997). Littermate wild-type lines were also established as potential strain controls (melan-a5 and -a6 from the *Mgrn1*$^{md\text{-}nc}$ stock and melan-a7 from the *Atrn*$^{mg\text{-}3J}$ stock); these resembled other black melanocyte lines. After passage 10, CT was removed from all cell lines without cessation of proliferation. Melan-a cells (Bennett et al., 1987) were grown in the same medium (no CT). Melan-a cells are functionally *Ink4a-Arf* null, expressing neither p16^{INK4A} nor ARF proteins (Sviderskaya et al., 2002).

Melanin and cell proliferation assays

Lyophilized samples of 0.5–1.0 x 10^6 melanocytes were processed for chemical analyses to detect the specific degradation product of eumelanin, pyrrole-2,3,5-tricarboxylic acid (PTCA), after permanganate oxidation (Ito and Fujita, 1985; Ito and Wakamatsu, 1994) and the specific degradation product of pheomelanin, 4-amino-3-hydroxyphenylalanine (4-AHP), after hydriodic acid hydrolysis (Ito and Fujita, 1985; Wakamatsu et al., 2002). Both products were quantified by HPLC. The amounts of eumelanin and pheomelanin were obtained by multiplying the amounts of PTCA and 4-AHP by conversion factors of 50 and nine respectively. For measurement of total melanin (Friedmann et al., 1990), cell pellets were resuspended in 100 μl NaOH (1 M) and diluted with 400 μl water. The OD_{472} was measured and converted to melanin content via a standard curve using synthetic melanin (Sigma). This was normalized to cell number.

To calculate cell doubling times, triplicate cultures were plated at the specified density on 3-cm dishes. When cells were nearly confluent, they were detached with trypsin-EDTA, counted in triplicate by hemocytometer, and replated at a recorded density. A growth curve was drawn from the relative population increase. Cell doubling time over 30 days' growth was calculated from the curve.

cAMP assays

Cellular cAMP concentrations were measured using the HitHunter™ cAMP assay kit (Amersham Biosciences, UK), according to the manufacturer's instructions with slight modifications. Cells were plated into 96-well plates at 2 x 10^4 cells/well, 100 μl medium/well and incubated at 37°C in normal culture conditions overnight. Medium was gently aspirated. Then, unless specified, cells were incubated in serum-free RPMI1640 with BSA (1 mg/ml) and 0, 10 or 100 nM ASIP at 37°C in a humidified atmosphere of 10% CO_2 for 30 min. To assess the effect of incubation of ASIP in medium, RPMI1640 containing 10% FBS and 100 nM ASIP was incubated under the same conditions for 12 h and this medium was applied in place of the medium with fresh ASIP. For cell stimulation, NDP-MSH (30 pM) and IBMX (1 mM) were added directly to the ASIP-containing medium and cells were incubated at 37°C for 30 min. The cells were lysed and processed according to the manufacturer's protocol. One hour after the last reaction step, the luminescence of each well was measured with a Synergy™ HT Multi-Mode microplate reader equipped with KC4 for Windows data-reduction software (Bio-Tek Instruments, VT, USA). The cAMP concentration in each sample was calculated by comparing relative luminescence of the sample with that of a cAMP standard.

Acknowledgements

We are grateful to Simon Hill for expert assistance in establishing the melan-e cell lines, and Marta Cantero for technical assistance with mice. Parts of the research were supported by Wellcome Trust program grants 064583 and 078327 to D.C.B. and E.V.S.; the Japan Society for the Promotion of Science KAKENHI (grants 20790808 to T.H. and 18591262 and 20591357 to K.W. and S.I.); a Grant-in-Aid from the Japanese Ministry of Health, Labour and Welfare (K.J.), the Spanish Ministry of Education and Science BFU2006-12185 (L.M.), the South West Academic Network (A.J.D. and E.V.S.), and NIH grant DK064265 (B.Y. and G.L.M.).

Supporting information

Additional Supporting Information may be found in the online version of this article:

Figure S1. Lack of morphological effect of ASIP on melan-e cells.

Figure S2. Reduction of visible pigmentation in melan-mg and melan-md cells grown with ASIP but not ASIP-YY.

Please note: Wiley-Blackwell are not responsible for the content or functionality of any supporting materials supplied by the authors. Any queries (other than missing material) should be directed to the corresponding author for the article.

References

Abdel-Malek, Z.A., Scott, M.C., Furumura, N., Lamoreux, M.L., Ollmann, M., Barsh, G.S., and Hearing, V.J. (2001). The melanocortin 1 receptor is the principal mediator of the effects of agouti signaling protein on mammalian melanocytes. J. Cell Sci. *114*, 1019–1024.

Aberdam, E., Bertolotto, C., Sviderskaya, E.V., de Thillot, V., Hemesath, T.J., Fisher, D.E., Bennett, D.C., Ortonne, J.P., and Ballotti, R. (1998). Involvement of microphthalmia in the inhibition of melanocyte lineage differentiation and of melanogenesis by Agouti signal protein. J. Biol. Chem. *273*, 19560–19565.

Barsh, G.S. (2006). Regulation of pigment type switching by agouti, melanocortin signaling, attractin and mahoganoid. In The Pigmentary System, 2nd edn J.J. Nordlund, R.E. Boissy, V.J. Hearing, R.A. King, W.S. Oetting, and J.P. Ortonne, eds (Massachusetts: Blackwell Publishing), pp. 395–409.

Bennett, D.C. (1989). Mechanisms of differentiation in melanoma cells and melanocytes. Environ. Health Perspect. *80*, 49–60.

Bennett, D.C., and Lamoreux, M.L. (2003). The color loci of mice–a genetic century. Pigment Cell Res. *16*, 333–344.

Bennett, D.C., Cooper, P.J., and Hart, I.R. (1987). A line of non-tumorigenic mouse melanocytes, syngeneic with the B16 melanoma and requiring a tumour promoter for growth. Int. J. Cancer *39*, 414–418.

Bertolotto, C., Abbe, P., Hemesath, T.J., Bille, K., Fisher, D.E., Ortonne, J.P., and Ballotti, R. (1998). Microphthalmia gene product as a signal transducer in cAMP-induced differentiation of melanocytes. J. Cell Biol. *142*, 827–835.

Buffey, J., Thody, A.J., Bleehen, S.S., and MacNeil, S. (1992). Alpha-melanocyte-stimulating hormone stimulates protein kinase C activity in murine B16 melanoma. J. Endocrinol. *133*, 333–340.

Candille, S.I., Kaelin, C.B., Cattanach, B.M., Yu, B., Thompson, D.A., Nix, M.A., Kerns, J.A., Schmutz, S.M., Millhauser, G.L., and Barsh, G.S. (2007). A β-defensin mutation causes black coat color in domestic dogs. Science *318*, 1418–1423.

Clément, K., Dubern, B., Mencarelli, M., Czernichow, P., Ito, S., Wakamatsu, K., Barsh, G., Vaisse, C., and Leger, J. (2008). Unexpected endocrine features and normal pigmentation in a young adult patient carrying a novel homozygous mutation in the POMC gene. J. Clin. Endocrinol. Metab. *93*, 4955–4962.

Costin, G.E., Vieira, W.D., Valencia, J.C., Rouzaud, F., Lamoreux, M.L., and Hearing, V.J. (2004). Immortalization of mouse melanocytes carrying mutations in various pigmentation genes. Anal. Biochem. *335*, 171–174.

Duhl, D.M.J., Stevens, M.E., Vrieling, H., Saxon, P.J., Miller, M.W., Epstein, C.J., and Barsh, G.S. (1994). Pleiotropic effects of the mouse lethal yellow (A^y) mutation explained by deletion of a maternally expressed gene and the simultaneous production of *agouti* fusion RNAs. Development *120*, 1695–1708.

Englaro, W., Rezzonico, R., Durand-Clément, M., Lallemand, D., Ortonne, J.P., and Ballotti, R. (1995). Mitogen-activated protein kinase pathway and AP-1 are activated during cAMP-induced melanogenesis in B-16 melanoma cells. J. Biol. Chem. *270*, 24315–24320.

Eves, P., Haycock, J., Layton, C. et al. (2003). Anti-inflammatory and anti-invasive effects of alpha-melanocyte-stimulating hormone in human melanoma cells. Br. J. Cancer *89*, 2004–2015.

Friedmann, P.S., Wren, F.E., and Matthews, J.N.S. (1990). Ultraviolet stimulated melanogenesis by human melanocytes is augmented by di-acyl glycerol but not TPA. J. Cell. Physiol. *142*, 334–341.

García-Borrón, J.C., Sánchez-Laorden, B.L., and Jiménez-Cervantes, C. (2005). Melanocortin-1 receptor structure and functional regulation. Pigment Cell Res. *18*, 393–410.

Graham, A., Wakamatsu, K., Hunt, G., Ito, S., and Thody, A.J. (1997). Agouti protein inhibits the production of eumelanin and phaeomelanin in the presence and absence of α-melanocyte stimulating hormone. Pigment Cell Res. *10*, 298–303.

He, L., Gunn, T.M., Bouley, D.M., Lu, X.Y., Watson, S.J., Schlossman, S.F., Duke-Cohan, J.S., and Barsh, G.S. (2001). A biochemical function for attractin in agouti-induced pigmentation and obesity. Nat. Genet. *27*, 40–47.

He, L., Eldridge, A.G., Jackson, P.K., Gunn, T.M., and Barsh, G.S. (2003). Accessory proteins for melanocortin signaling - Attractin and mahogunin. Ann. NY Acad. Sci. *994*, 288–298.

Hirobe, T., and Takeuchi, T. (1978). Changes of organelles associated with the differentiation of epidermal melanocytes in the mouse. J. Embryol. Exp. Morphol. *43*, 107–121.

Ito, S. (2003). The IFPCS presidental lecture: a chemist's view of melanogenesis. Pigment Cell Res. *16*, 230–236.

Ito, S., and Fujita, K. (1985). Microanalysis of eumelanin and pheomelanin in hair and melanomas by chemical degradation and liquid chromatography. Anal. Biochem. *144*, 527–536.

Ito, S., and Wakamatsu, K. (1994). An improved modification of permanganate oxidation of eumelanin that gives a constant yield of pyrrole-2,3,5-tricarboxylic acid. Pigment Cell Res. *7*, 141–144.

Ito, S., and Wakamatsu, K. (2008). Chemistry of mixed melanogenesis – pivotal roles of dopaquinone. Photochem. Photobiol. *84*, 582–592.

Jimbow, K., Hua, C., Gomez, P.F., Hirosaki, K., Shinoda, K., Salopek, T.G., Matsusaka, H., Jin, H.Y., and Yamashita, T. (2000). Intracellular vesicular trafficking of tyrosinase gene family protein in eu- and pheomelanosome biogenesis. Pigment Cell Res. *13*(Suppl 8), 110–117.

Land, E.J., Ito, S., Wakamatsu, K., and Riley, P.A. (2003). Rate constants for the first two chemical steps of eumelanogenesis. Pigment Cell Res. *16*, 487–493.

Le Pape, E., Wakamatsu, K., Ito, S., Wolber, R., and Hearing, V.J. (2008). Regulation of eumelanin/pheomelanin synthesis and visible pigmentation in melanocytes by ligands of the melanocortin 1 receptor. Pigment Cell Melanoma Res. *21*, 477–486.

Le Pape, E., Passeron, T., Giubellino, A., Valencia, J.C., Wolber, R., and Hearing, V.J. (2009). Microarray analysis sheds light on the dedifferentiating role of agouti signal protein in murine melanocytes via the Mc1r. Proc. Natl Acad. Sci. USA *106*, 1802–1807.

Levy, C., Khaled, M., and Fisher, D.E. (2006). MITF: master regulator of melanocyte development and melanoma oncogene. Trends Mol. Med. *12*, 406–414.

McNulty, J.C., Jackson, P.J., Thompson, D.A., Chai, B., Gantz, I., Barsh, G.S., Dawson, P.E., and Millhauser, G.L. (2005). Structures of the agouti signaling protein. J. Mol. Biol. *346*, 1059–1070.

Millar, S.E., Miller, M.W., Stevens, M.E., and Barsh, G.S. (1995). Expression and transgenic studies of the mouse *agouti* gene provide insight into the mechanisms by which mammalian coat color patterns are generated. Development *121*, 3223–3232.

Mountjoy, K.G., Kong, P.L., Taylor, J.A., Willard, D.H., and Wilkison, W.O. (2001). Melanocortin receptor-mediated mobilization of intracellular free calcium in HEK293 cells. Physiol. Genomics *5*, 11–19.

Ollmann, M.M., Lamoreux, M.L., Wilson, B.D., and Barsh, G.S. (1998). Interaction of Agouti protein with the melanocortin 1 receptor in vitro and in vivo. Genes Dev. *12*, 316–330.

Ozeki, H., Ito, S., Watamatsu, K., and Hirobe, T. (1995). Chemical characterization of hair melanins in various coat-color mutants of mice. J. Invest. Dermatol. *105*, 361–366.

Park, H.Y., Wu, C., Yonemoto, L., Murphy-Smith, M., Wu, H., Stachur, C.M., and Gilchrest, B.A. (2006). MITF mediates cAMP-induced protein kinase C-beta expression in human melanocytes. Biochem. J. *395*, 571–578.

Robbins, L.S., Nadeau, J.H., Johnson, K.R., Kelly, M.A., Roselli-Rehfuss, L., Baack, E., Mountjoy, K.G., and Cone, R.D. (1993). Pigmentation phenotypes of various extension locus alleles results from point mutations that alter MSH receptor function. Cell *72*, 827–834.

Sakai, C., Ollmann, M., Kobayashi, T., Abdel-Malek, Z., Muller, J., Vieira, W.D., Imokawa, G., Barsh, G.S., and Hearing, V.J. (1997). Modulation of murine melanocyte function *in vitro* by agouti signal protein. EMBO J. *16*, 3544–3552.

Sanchez-Mas, J., Hahmann, C., Gerritsen, I., García-Borrón, J.C., and Jiménez-Cervantes, C. (2004). Agonist-independent, high constitutive activity of the human melanocortin 1 receptor. Pigment Cell Res. *17*, 386–395.

Slominski, A., Plonka, P.M., Pisarchik, A., Smart, J.L., Tolle, V., Wortsman, J., and Low, M.J. (2005). Preservation of eumelanin hair pigmentation in proopiomelanocortin-deficient mice on a nonagouti (a/a) genetic background. Endocrinology *146*, 1245–1253.

Smalley, K., and Eisen, T. (2000). The involvement of p38 mitogen-activated protein kinase in the alpha-melanocyte stimulating hormone (alpha-MSH)-induced melanogenic and anti-proliferative effects in B16 murine melanoma cells. FEBS Lett. *476*, 198–202.

Sviderskaya, E.V., Wakeling, W.F., and Bennett, D.C. (1995). A cloned, immortal line of murine melanoblasts inducible to differentiate to melanocytes. Development *121*, 1547–1557.

Sviderskaya, E.V., Bennett, D.C., Ho, L., Bailin, T., Lee, S.T., and Spritz, R.A. (1997). Complementation of hypopigmentation in